SIAM J. NUMER. ANAL.
Vol. 51, No. 1, pp. 377–399

A MULTISCALE MORTAR MIXED SPACE BASED ON HOMOGENIZATION FOR HETEROGENEOUS ELLIPTIC PROBLEMS*

TODD ARBOGAST† AND HAILONG XIAO‡

Abstract. We consider a second order elliptic problem with a heterogeneous coefficient written in mixed form. The nonoverlapping mortar domain decomposition method is efficient in parallel if the mortar interface coupling space has a restricted number of degrees of freedom. In the heterogeneous case, we define a new multiscale mortar space that incorporates purely local information from homogenization theory to better approximate the solution along the interfaces with just a few degrees of freedom. In the case of a locally periodic heterogeneous coefficient of period ε, we prove that the new method achieves both optimal order error estimates in the discretization parameters and good approximation when ε is small. Moreover, we present three numerical examples to assess its performance when the coefficient is not obviously locally periodic. We show that the new mortar method works well, and better than polynomial mortar spaces.

Key words. nonoverlapping domain decomposition, mixed method, multiscale finite element, multiscale mortar, homogenization, convergence

AMS subject classifications. 65N15, 65N30, 65N55, 76M50, 76S05

DOI. 10.1137/120874928

1. Introduction.

Domain decomposition methods for partial differential equations have been developed as a linear solver strategy that increases parallelism. We consider a nonoverlapping domain decomposition approach [18] to solving a second order elliptic problem in mixed form [11, 34, 10] with a heterogeneous coefficient. We fully resolve the problem within the subdomains, and glue these together with reduced coupling through a relatively small mortar finite element space [9, 6, 7]. Recently, one of the current authors noted a microstructure result from homogenization theory, and used it to design new multiscale mixed finite elements [3, 4]. In this paper, we extend this idea to the domain decomposition context by defining and analyzing a new multiscale mortar space based on this homogenization microstructure result. Our work can be viewed in either of two complementary ways.

First, in a domain decomposition approach, one can view the subdomains as coarse elements in a multiscale finite element method [7, 16, 31, 4]; thus, we define, in essence, a new multiscale finite element, generalizing the approach in [3]. In the case of a two-scale coefficient, we prove that the method has optimal order error estimates with respect to the discretization parameters, and gives a good approximation with respect to the heterogeneity variability ε. This is notable for a purely local method, since generally local methods exhibit severe numerical resonance effects due to imposition of local boundary conditions [21, 22, 15, 12, 5, 2].

*Received by the editors April 25, 2012; accepted for publication (in revised form) October 9, 2012; published electronically February 12, 2013. This work was supported as part of the Center for Frontiers of Subsurface Energy Security, an Energy Frontier Research Center funded by the U.S. Department of Energy, Office of Science, Office of Basic Energy Sciences under Award DE-SC0001114.
http://www.siam.org/journals/sinum/51-1/87492.html
†Department of Mathematics, and Institute for Computational Engineering and Sciences, University of Texas, Austin, TX 78712-1229 (arbogast@ices.utexas.edu).
‡Institute for Computational Engineering and Sciences, University of Texas, Austin, TX 78712-1229 (xiaohl@ices.utexas.edu).

Second, our work can be viewed as an approximate nonoverlapping domain decomposition linear solver for parallel computation. In recent years, there has been a great deal of interest in merging ideas from multiscale finite elements and linear solver technologies such as domain decomposition and multigrid. Included are the works [28, 1, 37, 25, 19, 29, 24, 30, 14, 35]. The equations within the subdomains can be treated independently in parallel. The mortar ties the computation together, and is not naturally parallelizable. The use of fewer degrees of freedom in the mortar coupling space in our method gives rise to a smaller coarse problem, which increases the overall parallel efficiency of an iterative method.

To fix ideas, we consider a simple linear second order elliptic equation in both a domain decomposition setting and a mixed form. Let $\Omega \subset \mathbb{R}^d$, $d = 2, 3$, be the problem domain, decomposed into n nonoverlapping subdomains Ω_i, $i = 1, 2, \dots, n$, of maximal diameter L. The unknowns are *pressure* p and *velocity* $\mathbf{u}$, and we write p_i and $\mathbf{u}_i$ for their restrictions to Ω_i (or their traces on $\partial\Omega_i$). If ν and ν_i are the outer unit normals to $\partial\Omega$ and $\partial\Omega_i$, we have the problem

$$\mathbf{u} = -a_\varepsilon \nabla p \quad \text{in } \Omega_i, \tag{1.1}$$

$$\nabla \cdot \mathbf{u} = f \quad \text{in } \Omega_i, \tag{1.2}$$

$$p_i = p_j \quad \text{on } \partial\Omega_i \cap \partial\Omega_j \equiv \Gamma_{ij}, \tag{1.3}$$

$$\mathbf{u}_i \cdot \nu_i + \mathbf{u}_j \cdot \nu_j = 0 \quad \text{on } \Gamma_{ij}, \tag{1.4}$$

$$\mathbf{u} \cdot \nu = 0 \quad \text{on } \partial\Omega, \tag{1.5}$$

where a_ε is a tensor, uniformly positive definite and bounded, called the *permeability* in porous medium applications, and $f \in L^2(\Omega)$. It is assumed to vary on a fine scale $\varepsilon < L$. The restriction to a homogeneous Neumann boundary condition is purely for simplicity of exposition, and other boundary conditions could equally well be imposed.

In this paper, we first review in section 2 the standard mortar mixed finite element method. Based on the affect of the scale ε on the solution quality, in section 3 we motivate and define a new mortar space of functions within which to approximate the pressure on each Γ_{ij} using homogenization theory. Our new mortar space is based on polynomials, but it is itself nonpolynomial. Our convergence analysis is given in section 4, and it is based on comparison to the homogenized solution in the locally periodic setting of two-scale separation (see (3.7)). In this case, we quantify the dependence of the approximation error on the discretization parameters and ε (see Theorem 4.1). The proof makes strong use of a special mixed method projection operator Π_0 and a careful estimate of the interface error. Three numerical tests are given in section 5. Although our new mortar space was designed and analyzed based on homogenization, its definition and use do not require a locally periodic permeability. Therefore, our numerical tests emphasize nonperiodic permeability fields. We find that the new mortar space performs better overall, and often dramatically so, than simply using polynomial mortar approximating spaces. Finally, a summary and concluding remarks are given in section 6.

To fix some of our notation, for $\omega \subset \Omega$, let $\|\cdot\|_{k,p,\omega}$ denote the norm of the Sobolev space $W^{k,p}(\omega)$ of k times differentiable functions in $L^p(\omega)$, $1 \le p \le \infty$. Similarly, $\|\cdot\|_{k,\omega}$ is the norm of the Hilbert space $H^k(\omega) = W^{k,2}(\omega)$. Also, $H(\text{div};\omega) = \{\mathbf{v} \in L^2(\omega) : \nabla\cdot\mathbf{v} \in L^2(\omega)\}$ has the usual norm $\|\mathbf{v}\|_{H(\text{div};\omega)} = \{\|\mathbf{v}\|_{0,\omega}^2 + \|\nabla\cdot\mathbf{v}\|_{0,\omega}^2\}^{1/2}$. We write $(\cdot,\cdot)_\omega$ for the $L^2(\omega)$ or $\big(L^2(\omega)\big)^d$ inner product, and $\langle\cdot,\cdot\rangle_{\partial\omega}$ for the duality pairing on boundaries and interfaces, where the pairing may be between two functions in L^2 or between elements of $H^{1/2}$ and $H^{-1/2}$, in either order. We omit ω in the notation if it is Ω.

2. The mortar mixed finite element method. In this section, we review the basics of the mortar mixed method [18, 38, 6, 7]. To incorporate the boundary condition on the velocity, for each subdomain i, define $\mathbf{V}_i = \{\mathbf{v} \in H(\mathrm{div};\Omega_i) : \mathbf{v}\cdot\nu|_{\partial\Omega\cap\partial\Omega_i} = 0\}$ and $\mathbf{V} = \bigoplus_{i=1}^n \mathbf{V}_i$. Moreover, let $W_i = L^2(\Omega_i)$ and $W = \{w \in L^2(\Omega) : \int_\Omega w\,dx = 0\}$. We formulate the variational form of (1.1)–(1.5) in the sense of domain decomposition as follows: Find $\mathbf{u}\in\mathbf{V}$, $p \in W$, and $\lambda = p \in M = H^{1/2}(\Gamma)$ ($\Gamma = \bigcup_{i,j}\Gamma_{ij}, \Gamma_i = \partial\Omega_i \bigcap \Gamma$) such that for $1 \le i \le n$,

$$(a_\varepsilon^{-1}\mathbf{u},\mathbf{v})_{\Omega_i} - (p,\nabla\cdot\mathbf{v})_{\Omega_i} + \langle\lambda,\mathbf{v}\cdot\nu_i\rangle_{\Gamma_i} = 0 \qquad \forall\,\mathbf{v}\in\mathbf{V}_i, \tag{2.1}$$

$$(\nabla\cdot\mathbf{u}, w)_{\Omega_i} = (f,w)_{\Omega_i} \quad \forall\, w \in W_i, \tag{2.2}$$

$$\sum_{i=1}^n \langle \mathbf{u}\cdot\nu_i,\mu\rangle_{\Gamma_i} = 0 \qquad \forall\,\mu\in M. \tag{2.3}$$

2.1. Discrete formulation. Let $\mathcal{T}_{h,i}$ be a conforming, quasi-uniform, finite element partition of Ω_i. Let h_i denote the maximum element diameter of the partition $\mathcal{T}_{h,i}$ and $h = \max_i h_i$. Define $\mathcal{T}_h = \bigcup_{i=1}^n \mathcal{T}_{h,i}$ as the finite element partition over the entire domain Ω. Let $\mathbf{V}_{h,i}\times W_{h,i} \subset \mathbf{V}_i \times W_i$ denote any of the usual inf-sup stable mixed finite element spaces for which $\nabla\cdot\mathbf{V}_{h,i} = W_{h,i}$ [11, 34], e.g., the Raviart–Thomas spaces [33]. Define $\mathbf{V}_h = \bigoplus_{i=1}^n \mathbf{V}_{h,i}$ and $W_h = \bigoplus_{i=1}^n W_{h,i}/\mathbb{R}$ for the global discrete velocity and pressure. Denote by $\mathcal{T}_{H,ij}$ a quasi-uniform finite element partition of Γ_{ij}, with maximal diameter of H_{ij} and $H = \max_{1\le i,j\le n} H_{ij}$. Let $M_{H,ij} \subset L^2(\Gamma_{ij})$ be the local mortar finite element space and let $M_H = \bigoplus_{i\ne j} M_{H,ij}$ be the entire coarse mortar finite element space that we will define later.

The discrete variational form can be formulated as follows: Find $\mathbf{u}_h \in \mathbf{V}_h$, $p_h \in W_h$, $\lambda_H \in M_H$ such that for $1 \le i \le n$,

$$(a_\varepsilon^{-1}\mathbf{u}_h,\mathbf{v})_{\Omega_i} - (p_h,\nabla\cdot\mathbf{v})_{\Omega_i} + \langle\lambda_H,\mathbf{v}\cdot\nu_i\rangle_{\Gamma_i} = 0 \qquad \forall\,\mathbf{v}\in\mathbf{V}_{h,i}, \tag{2.4}$$

$$(\nabla\cdot\mathbf{u}_h, w)_{\Omega_i} = (f,w)_{\Omega_i} \quad \forall\, w \in W_{h,i}, \tag{2.5}$$

$$\sum_{i=1}^n \langle \mathbf{u}_h\cdot\nu_i,\mu\rangle_{\Gamma_i} = 0 \qquad \forall\mu\in M_H. \tag{2.6}$$

We remark that the mesh is allowed to be nonmatching across some Γ_{ij}, in which case the method gives a nonconforming approximation.

A unique discrete solution exists provided only that a technical condition is met, which is given below in (A.1) and implied by our Assumption 4.1 given later. Throughout the paper, we will tacitly make this assumption.

2.2. The coarse interface problem. Define the bilinear form $d_H : M_H \times M_H \to \mathbb{R}$ and linear functional $g_H : M_H \to \mathbb{R}$ by

$$d_H(\lambda,\mu) = -\sum_{i=1}^n \langle \mathbf{u}_h^*(\lambda)\cdot\nu_i,\mu\rangle_{\Gamma_i},$$

$$g_H(\mu) = \sum_{i=1}^n \langle \bar{\mathbf{u}}_h\cdot\nu_i,\mu\rangle_{\Gamma_i},$$

where $(\mathbf{u}_h^*(\lambda), p_h^*(\lambda)) \in \mathbf{V}_h \times W_h$ solves (λ given, $f = 0$)

$$(a_\varepsilon^{-1}\mathbf{u}_h^*(\lambda),\mathbf{v})_{\Omega_i} - (p_h^*(\lambda),\nabla\cdot\mathbf{v})_{\Omega_i} = -\langle\lambda,\mathbf{v}\cdot\nu_i\rangle_{\Gamma_i} \quad \forall\,\mathbf{v}\in\mathbf{V}_{h,i},$$
$$(\nabla\cdot\mathbf{u}_h^*(\lambda), w)_{\Omega_i} = 0 \qquad \forall\, w\in W_{h,i},$$

and $(\bar{\mathbf{u}}_h, \bar{p}_h) \in \mathbf{V}_h \times W_h$ solves ($\lambda = 0$, f given)

$$(a_\varepsilon^{-1}\bar{\mathbf{u}}_h, \mathbf{v})_{\Omega_i} - (\bar{p}_h, \nabla\cdot\mathbf{v})_{\Omega_i} = 0 \qquad \forall\, \mathbf{v} \in \mathbf{V}_{h,i},$$
$$(\nabla\cdot\bar{\mathbf{u}}_h, w)_{\Omega_i} = (f, w)_{\Omega_i} \qquad \forall\, w \in W_{h,i}.$$

The equivalent coarse variational problem is as follows: Find $\lambda_H \in M_H$ such that

$$d_H(\lambda_H, \mu) = g_h(\mu) \quad \forall\, \mu \in M_H. \tag{2.7}$$

In fact, as shown in [38, 6], d_H is symmetric and positive definite, and the interface problem (2.7) generates the solution of (2.4)–(2.6) via

$$\mathbf{u}_h = \mathbf{u}_h^*(\lambda_H) + \bar{\mathbf{u}}_h, \quad p_h^\dagger = p_h^*(\lambda_H) + \bar{p}_h, \quad p_h = p_h^\dagger - \frac{1}{|\Omega|}\int_\Omega p_h^\dagger\, dx.$$

As noted in the introduction, we can view the solution of the interface problem (2.7) in at least two equivalent ways. In the traditional view [18, 6], the interface problem is solved iteratively using conjugate gradients. Given λ_H^q, one solves the n subdomain problems for $\mathbf{u}_h^*(\lambda_H^q)$, computes the residual, and updates the mortar to λ_H^{q+1} until convergence is achieved. In the alternative view [7, 16, 4], one forms multiscale finite elements over the subdomains. We first find a basis for M_H. For each Γ_{ij}, we have a set of mortar basis functions λ_q^{ij} which generate the multiscale basis $\mathbf{u}_h^*(\lambda_q^{ij})$ over the "coarse elements" Ω_i and Ω_j. From these, we form the interface matrix in (2.7) directly, and solve the system in any reasonable way.

It remains to define a suitable space M_H, preferably with as few degrees of freedom as possible. If we use inf-sup stable mixed finite element spaces giving approximation of order $\mathcal{O}(h^k)$ for $\mathbf{u}$ and $\mathcal{O}(h^\ell)$ for p, and if we use a high order mortar space M_H of piecewise (continuous or discontinuous) polynomials of degree $m-1$ over the coarse mortar mesh $\mathcal{T}_{H,ij}$ on each Γ_{ij}, then from [7] we have the following a priori estimates.

THEOREM 2.1. *Under Assumption* 4.1*, there exists C, independent of h and H, such that for $1 \le r \le k$, $0 \le s \le \ell$, and $0 < t \le m$,*

$$\|\nabla\cdot(\mathbf{u}-\mathbf{u}_h)\|_0 \le C\|f\|_s h^s,$$
$$\|\mathbf{u}-\mathbf{u}_h\|_0 \le C\big\{\|\mathbf{u}\|_r h^r + \|p\|_{t+1/2}H^{t-1/2} + \|\mathbf{u}\|_{r+1/2}h^r H^{1/2}\big\},$$
$$\|p-p_h\|_0 \le C\big\{\|p\|_s h^s + \|p\|_{t+1/2}H^{t+1/2} + \|f\|_s h^s H + \|\mathbf{u}\|_r h^r H + \|\mathbf{u}\|_{r+1/2}h^r H^{3/2}\big\}.$$

A coarse mesh and a higher order approximation space can achieve a given level of accuracy with fewer degrees of freedom than a fine mesh and a low order approximation [7]. If the solution were to vary only on the coarse scale, we would simply take m sufficiently large that $h^k \sim H^{m-1/2}$.

3. The homogenization-based mortar mixed space. For a highly oscillating medium permeability a_ε with a characteristic length scale ε, the gradient of a function also depends on ε, i.e.,

$$\|\nabla p\|_0 = \mathcal{O}(\varepsilon^{-1}) \quad \text{and} \quad \|D^k p\|_0 = \mathcal{O}(\varepsilon^{-k}),$$

and similarly for $\mathbf{u}$. Then, the velocity and pressure error estimates in Theorem 2.1 become

$$\|\mathbf{u}-\mathbf{u}_h\|_0 \le C\big\{(h/\varepsilon)^r + (H/\varepsilon)^{t-1/2}/\varepsilon + (h/\varepsilon)^r(H/\varepsilon)^{1/2}\big\},$$
$$\|p-p_h\|_0 \le C\big\{(h/\varepsilon)^s[1+H] + (H/\varepsilon)^{t+1/2} + (h/\varepsilon)^r[1+(H/\varepsilon)^{1/2}]H\big\},$$

which also depend on ε. This suggests that the mesh size H of the mortar space should satisfy $H < \varepsilon$ to fully resolve the problem. However, for a multiscale finite element method, the relation between the fine scale h, the coarse scale H, and the characteristic length scale ε should be $h < \varepsilon < H$. Therefore, we develop a new technique to address this problem.

3.1. The interface error in the mortar method. We define the space of weakly continuous velocities [6]

$$\mathbf{V}_{h,0} = \left\{ \mathbf{v} \in \mathbf{V}_h : \sum_{i=1}^{n} \langle \mathbf{v}|_{\Omega_i} \cdot \nu_i, \mu \rangle_{\Gamma_i} = 0 \ \forall \mu \in M_H \right\}. \tag{3.1}$$

Then, instead of (2.1)–(2.3), we form an equivalent problem without λ_H: Find $\mathbf{u}_h \in \mathbf{V}_{h,0}$ and $p \in W_h$ such that

$$(a_\varepsilon^{-1}\mathbf{u}_h, \mathbf{v}) - \sum_{i=1}^{n} (p_h, \nabla \cdot \mathbf{v})_{\Omega_i} = 0 \qquad \forall \mathbf{v} \in \mathbf{V}_{h,0}, \tag{3.2}$$

$$\sum_{i=1}^{n} (\nabla \cdot \mathbf{u}_h, w)_{\Omega_i} = (f, w) \quad \forall w \in W_h. \tag{3.3}$$

If we work directly on the weakly continuous velocity space, subtracting (2.1)–(2.2) by (3.2)–(3.3), we obtain the equations for the error (recalling $p = \lambda$ on Γ)

$$(a_\varepsilon^{-1}(\mathbf{u} - \mathbf{u}_h), \mathbf{v}) - \sum_{i=1}^{n} \left[(p - p_h, \nabla \cdot \mathbf{v})_{\Omega_i} - \langle p, \mathbf{v} \cdot \nu_i \rangle_{\Gamma_i} \right] = 0 \quad \forall \mathbf{v} \in \mathbf{V}_{h,0}, \tag{3.4}$$

$$\sum_{i=1}^{n} (\nabla \cdot (\mathbf{u} - \mathbf{u}_h), w)_{\Omega_i} = 0 \quad \forall w \in W_h. \tag{3.5}$$

We observe that the velocity and pressure errors depend on the term $\langle p, \mathbf{v} \cdot \nu_i \rangle_{\Gamma_i}$. Since $\mathbf{v}$ is in the weakly continuous space,

$$\langle p, \mathbf{v} \cdot \nu_i \rangle_{\Gamma_i} = \langle p - \mu, \mathbf{v} \cdot \nu_i \rangle_{\Gamma_i} \quad \forall \mu \in M_H. \tag{3.6}$$

This suggests that we should define the mortar space so that this term will be small. We next use homogenization theory to make a better choice of the mortar space than piecewise polynomials.

3.2. The homogenization-based mortar space. For the rest of this section and throughout the next, we assume $a_\varepsilon(x)$ has two separated scales. Specifically, we suppose that

$$a_\varepsilon(x) = a(x, x/\varepsilon), \tag{3.7}$$

where $a(x, y)$ is a function of a slowly varying variable x and a fast varying variable y. Moreover, we suppose that $a(x, y)$ is periodic in y with the unit cell $\mathbf{Y} = [0, 1]^d$ as its period. We will remove this assumption for the numerical results of section 5. The two-scale separation assumption (3.7) is used here in this section only heuristically to motivate and define the new mortar method (up to treatment of the so-called cell problems, which is discussed in section 5), and in section 4 to provide some mathematical support for the accuracy of the method.

From standard homogenization theory [8, 23, 5], we have the cell problems

$$-\nabla_y \cdot \big[a(x,y)\big(\nabla_y \omega_k(x,y) + \mathbf{e}_k\big)\big] = 0 \quad \text{in } \Omega \times \mathbf{Y},\ k = 1,\dots,d,$$

where $\mathbf{e}_k$ is the standard unit vector in $\mathbb{R}^d$, which are used to define the homogenized tensor $a_0(x)$ as

$$a_{0,ij}(x) = \int_{\mathbf{Y}} a(x,y)\left(\delta_{ij} + \frac{\partial \omega_j(x,y)}{\partial y_i}\right) dy, \quad i,j = 1,\dots,d.$$

The homogenized problem is formulated as follows: Find p_0 and $\mathbf{u}_0$ such that

$$\mathbf{u}_0 = -a_0 \nabla p_0 \quad \text{in } \Omega, \tag{3.8}$$

$$\nabla \cdot \mathbf{u}_0 = f \quad \text{in } \Omega, \tag{3.9}$$

$$\mathbf{u}_0 \cdot \nu = 0 \quad \text{on } \partial\Omega. \tag{3.10}$$

From [23, 27, 5], we have the following estimate of the homogenization error, wherein and henceforth $\boldsymbol{\omega} = (\omega_1, \dots, \omega_d)^T$.

LEMMA 3.1. *Let the* first order corrector *be defined by*

$$p_\varepsilon^1(x) = p_0(x) + \varepsilon \boldsymbol{\omega}(x, x/\varepsilon) \cdot \nabla p_0(x). \tag{3.11}$$

If $p_0 \in H^2(\Omega)$ *solves* (3.8)–(3.10)*, then there is some constant* C*, depending on the solutions to the cell problems but not on* ε*, such that*

$$\|p - p_\varepsilon^1\|_0 \le C\varepsilon \|p_0\|_2. \tag{3.12}$$

Moreover, if $p_0 \in H^2(\Omega) \cap W^{1,\infty}(\Omega)$*, then*

$$\|\nabla(p - p_\varepsilon^1)\|_0 \le C\big\{\varepsilon \|\nabla p_0\|_1 + \sqrt{\varepsilon}\, \|\nabla p_0\|_{0,\infty}\big\}. \tag{3.13}$$

Although the solution p of (2.1)–(2.3) does not itself vary only on a coarse scale, it is a fixed operator of a coarse-scale function p_0. Thus we should approximate

$$\lambda(x) = p(x) \approx p_\varepsilon^1(x) = \big(1 + \varepsilon \boldsymbol{\omega}(x, x/\varepsilon) \cdot \nabla\big) p_0(x) \approx \big(1 + \varepsilon \boldsymbol{\omega}(x, x/\varepsilon) \cdot \nabla\big) q(x),$$

where $q(x)$ is a piecewise polynomial. This leads us to define a new multiscale mortar space, using piecewise polynomials. However, to approximate λ properly, one needs to apply the approximation not on Γ_{ij}, but on Γ_{ij}^*, an extension in the normal direction into $\overline{\Omega_i \cap \Omega_j}$. We therefore define $\mathcal{T}_{H,ij}^*$ to be the extended mesh and $\mathbb{P}_{m-1}(\mathcal{T}_{H,ij}^*)$ to be the piecewise (continuous or discontinuous) polynomials of degree $m-1$ defined over the interface mesh $\mathcal{T}_{H,ij}$ and extended in the normal direction of the same degree. We call $\mathbb{P}_{m-1}(\mathcal{T}_{H,ij}^*)$ the *generating polynomial space* for the mortar space, and we define

$$\begin{aligned} M_H &= \big\{\lambda \in L^2(\Gamma) : \lambda\big|_{e^*\cap\Gamma_{ij}} = \big(1 + \varepsilon \boldsymbol{\omega}(x, x/\varepsilon) \cdot \nabla\big) q\big|_{e^*\cap\Gamma_{ij}}, \\ &\qquad\qquad q \in \mathbb{P}_{m-1}(\mathcal{T}_{H,ij}^*),\ e^* \in \mathcal{T}_{H,ij}^*\big\} \\ &= \big\{\lambda \in L^2(\Gamma) : \lambda\big|_{\Gamma_{ij}} = \big(1 + \varepsilon \boldsymbol{\omega}(x, x/\varepsilon) \cdot \nabla_H\big) q\big|_{\Gamma_{ij}},\ q \in \mathbb{P}_{m-1}(\mathcal{T}_{H,ij}^*)\big\}, \end{aligned} \tag{3.14}$$

wherein the modified polynomials were restricted back to Γ, and ∇_H is the discrete, piecewise gradient. Moreover, $M_{H,ij}$ is M_H restricted to Γ_{ij}.

A simple example in two dimensions is instructive. Suppose that each Γ_{ij} is straight, and that we use only a single finite element over it, which we can map to $[0, H]$. Let x denote the coordinate in $[0, H]$, and let $y \in [-\eta, \eta]$ denote the normal coordinate into the domain (for some small η). If we choose for q a linear polynomial,

$$q(x, y) = \alpha + \beta x + \gamma y,$$

then the resulting homogenization-based element, restricted to $y = 0$, is

$$\lambda_H(x) = \alpha + \beta\big[x + \varepsilon\omega_1\big((x,0),(x,0)/\varepsilon\big)\big] + \gamma\varepsilon\omega_2\big((x,0),(x,0)/\varepsilon\big).$$

That is, with a linear approximation, $\lambda \in M_H$ has three degrees of freedom on each edge (not two). Similarly, in three dimensions, λ has four degrees of freedom on each face.

4. Convergence results. In this section we consider the convergence of the numerical approximation with respect to the relevant scales in the problem. We do this under the two-scale separation hypothesis (3.7), and so the results do not strictly apply to the general case of heterogeneous permeability a_ε. Nevertheless, our analysis provides support that the method provides an accurate approximation. The next section on numerical results will demonstrate good approximation in the general case.

The largest scale is associated to the size of the domain Ω, which we assume is normalized to one. The constants in our error bounds may depend on Ω. The next largest scale is L, which is associated to the size of the subdomains Ω_i. We assume that the subdomains are of a similar size and shape. Precisely, we assume that there are constants c_1 and c_2 such that each Ω_i contains a ball of radius c_1L and that each is contained in a ball of radius c_2L. Thus the relevant scales in our analysis are

$$h < \varepsilon < H \leq L \leq 1,$$

and the constants in our error bounds will not depend on these.

We need an assumption about the interface mesh and mortar space. To state it, for each domain Ω_i, we need to define the L^2 projection operator $\mathcal{Q}_{h,i} : L^2(\partial\Omega_i) \to \mathbf{V}_{h,i} \cdot \nu_i|_{\partial\Omega_i}$ such that for all $\phi \in L^2(\partial\Omega_i)$,

$$\langle \phi - \mathcal{Q}_{h,i}\phi, \mathbf{v} \cdot \nu_i\rangle_{\partial\Omega_i} = 0 \quad \forall\, \mathbf{v} \in \mathbf{V}_{h,i}. \tag{4.1}$$

Assumption 4.1. There exists a constant C, independent of h, H, L, and ε, such that for all $\mu \in M_H$ and all Γ_{ij},

$$\|\mu\|_{0,\Gamma_{ij}} \leq C\big\{\|\mathcal{Q}_{h,i}\mu\|_{0,\Gamma_{ij}} + \|\mathcal{Q}_{h,j}\mu\|_{0,\Gamma_{ij}}\big\}. \tag{4.2}$$

This assumption is not too restrictive: In [38, 32] it is shown that it is easily satisfied in practice for polynomial mortar spaces. We show that it is satisfied in a reasonable situation in Appendix A.

We will make use of the L^2 projection, defined for any $\phi \in L^2(\Omega)$ as $\hat{\phi} \in W_h$, satisfying

$$(\phi - \hat{\phi}, w) = 0 \quad \forall\, w \in W_h,$$

for which it is well known that

$$\|\phi - \hat{\phi}\|_0 \leq C\|\phi\|_s h^s, \quad 0 \leq s \leq \ell. \tag{4.3}$$

Recall that we use quasi-uniform, affine finite element partitions and inf-sup stable mixed finite element spaces such that $\nabla \cdot \mathbf{V}_h = W_h$ and giving approximation of order $\mathcal{O}(h^k)$ for $\mathbf{u}$ and $\mathcal{O}(h^\ell)$ for p, and we use a mortar space M_H based on homogenization using piecewise (continuous or discontinuous) generating polynomials giving approximation of order $\mathcal{O}(H^m)$. We have the following bounds on the velocity and pressure errors.

THEOREM 4.1. *Suppose both Assumption* 4.1 *and the two-scale separation assumption* (3.7) *hold. Then there exists a constant C, independent of h, H, L, and ε, such that for $1 \le r \le k$, $0 \le s \le \ell$, and $0 < t \le m$,*

$$\|\nabla \cdot (\mathbf{u} - \mathbf{u}_h)\|_0 \le C\|f\|_s h^s, \tag{4.4}$$

$$\|p - p_h\|_0 \le \|\hat{p} - p_h\|_0 + C\|p\|_s h^s, \tag{4.5}$$

$$\begin{aligned}\|\mathbf{u} - \mathbf{u}_h\|_0 + \|\hat{p} - p_h\|_0 \le C\big\{ &\big[\|\mathbf{u}\|_r + \|\mathbf{u}\|_{r+1/2}((H+\varepsilon)/L)^{1/2}\big]h^r \\ &+ H^{t-1}(H+\varepsilon)(Lh)^{-1/2}\|p_0\|_{t+1/2} + \varepsilon\|p_0\|_2 + \varepsilon^{1/2}\|\nabla p_0\|_{0,\infty}\big\},\end{aligned} \tag{4.6}$$

$$\begin{aligned}\|\mathbf{u} - \mathbf{u}_h\|_0 + \|\hat{p} - p_h\|_0 \le C\big\{ &\|\mathbf{u}\|_r((H+\varepsilon)/L)^{1/2}h^{r-1/2} \\ &+ H^{t-1}(H+\varepsilon)(Lh)^{-1/2}\|p_0\|_{t+1/2} + \varepsilon\|p_0\|_2 + \varepsilon^{1/2}\|\nabla p_0\|_{0,\infty}\big\}.\end{aligned} \tag{4.7}$$

Moreover, if the generating polynomial space contains a C^1 subspace of approximation order $\mathcal{O}(H^m)$ over Γ, then

$$\begin{aligned}\|\mathbf{u} - \mathbf{u}_h\|_0 + \|\hat{p} - p_h\|_0 \le C\big\{ &\big[\|\mathbf{u}\|_r + \|\mathbf{u}\|_{r+1/2}((H+\varepsilon)/L)^{1/2}\big]h^r \\ &+ H^{t-3/2}(1+\varepsilon)L^{-1/2}\|p_0\|_{t+1/2} + \varepsilon\|p_0\|_2 + \varepsilon^{1/2}\|\nabla p_0\|_{0,\infty}\big\},\end{aligned} \tag{4.8}$$

$$\begin{aligned}\|\mathbf{u} - \mathbf{u}_h\|_0 + \|\hat{p} - p_h\|_0 \le C\big\{ &\|\mathbf{u}\|_r((H+\varepsilon)/L)^{1/2}h^{r-1/2} \\ &+ H^{t-3/2}(1+\varepsilon)L^{-1/2}\|p_0\|_{t+1/2} + \varepsilon\|p_0\|_2 + \varepsilon^{1/2}\|\nabla p_0\|_{0,\infty}\big\}.\end{aligned} \tag{4.9}$$

Estimate (4.4) follows in the usual way from (3.5), since $\nabla \cdot \mathbf{V}_h = W_h$. Estimate (4.5) follows from (4.3). The proof of the rest of the theorem is given below. It follows basically from [6, 7], with important modifications for estimating the mortar errors.

If $\varepsilon < H$, the estimate (4.6) is $\mathcal{O}(h^r + H^t h^{-1/2})$ in the discretization parameters h and H. This is formally of optimal order if h and H are comparable, since we expect $\mathcal{O}(h^r)$ for the subdomain approximation and $\mathcal{O}(H^{t-1/2})$ for the mortar (which loses 1/2 power due to the fact that the mortar is supported on an interface).

In terms of the characteristic length scale ε, again, the derivatives of $\mathbf{u}$ scale as ε^{-1}. However, p_0 is independent of ε and therefore varies only on a coarse scale. Thus, assuming the scales satisfy $h < \varepsilon < H \le L \le 1$, the estimate in the general case, (4.6) is

$$\|\mathbf{u} - \mathbf{u}_h\|_0 + \|\hat{p} - p_h\|_0 \le C\left\{ \left[\left(\frac{h}{\varepsilon}\right)^{r+1/2} + H^{t-1/2}\right]\sqrt{\frac{H}{Lh}} + \sqrt{\varepsilon}\right\},$$

and in the smooth generating polynomial space case, (4.8) is

$$\|\mathbf{u} - \mathbf{u}_h\|_0 + \|\hat{p} - p_h\|_0 \le C\left\{ \left(\frac{h}{\varepsilon}\right)^{r+1/2}\sqrt{\frac{H}{Lh}} + H^{t-2}\sqrt{\frac{H}{L}} + \sqrt{\varepsilon}\right\}.$$

These estimates do not degenerate as $H \to \varepsilon^+$. Moreover, all terms are small, except perhaps the factor $\sqrt{H/(Lh)}$. In practical application, the ratio $H/(Lh)$ should probably be bounded. Some restriction of this kind is to be expected, since it makes little sense to overresolve the subdomains by a tiny mesh spacing h without a reasonable resolution H of the mortar.

For the proof, we will need the following four mostly well-known results, with C independent of h, H, L, and ε, which we collect here for reference:

(4.10) $\|q\|_{r,\Gamma_{ij}} \le CL^{-1/2}\|q\|_{r+1/2,\Omega_i}, \quad 0 < r$ (trace theorem [20]);

(4.11) $\|\mathbf{v}\cdot\nu\|_{0,\partial\Omega_i} \le Ch^{-1/2}\|\mathbf{v}\|_{0,\Omega_i} \quad \forall \mathbf{v} \in \mathbf{V}_h \cup \mathbf{V}_{h,0}$ (local inverse inequality);

(4.12) $\langle q, \mathbf{v}\cdot\nu\rangle_{\partial\Omega_i} \le C\big\{\|q\|_{0,\Omega_i}\|\nabla\cdot\mathbf{v}\|_{0,\Omega_i} + \|\nabla q\|_{0,\Omega_i}\|\mathbf{v}\|_{0,\Omega_i}\big\}$ ($H(\text{div})$ trace theorem 1 [11]);

(4.13) $\langle q, \mathbf{v}\cdot\nu\rangle_{\partial\Omega_i} \le C\|q\|_{1/2,\partial\Omega_i}\|\mathbf{v}\|_{H(\text{div};\Omega_i)}$ ($H(\text{div})$ trace theorem 2 [11]).

4.1. A mixed method projection operator. Mixed method error analysis is facilitated by the introduction of a special vector-variable projection operator. We will define it as a modification of the standard Fortin projection [33, 11, 34] of smooth velocities to the discrete velocity space, which in our case is $\mathbf{V}_{h,0}$, the space of weakly continuous velocities defined in (3.1).

LEMMA 4.2. *Under Assumption* 4.1*, for* $\eta > 0$*, there exists a projection operator* $\Pi_0 : (H^\eta(\Omega)) \cap \mathbf{V} \to \mathbf{V}_{h,0}$ *such that*

$$(\nabla\cdot(\Pi_0\mathbf{v} - \mathbf{v}), w)_\Omega = 0 \quad \forall\, w \in W_h. \tag{4.14}$$

Moreover,

$$\|\Pi_0\mathbf{v} - \mathbf{v}\|_0 \le C\big\{\|\mathbf{v}\|_r + \|\mathbf{v}\|_{r+1/2}((H+\varepsilon)/L)^{1/2}\big\}h^r, \quad 1 \le r \le k, \tag{4.15}$$

$$\|\Pi_0\mathbf{v} - \mathbf{v}\|_0 \le C\|\mathbf{v}\|_r((H+\varepsilon)/L)^{1/2}h^{r-1/2}, \quad 1 \le r \le k. \tag{4.16}$$

This projection was introduced in [6] for standard polynomial mortar spaces. It was noted in [7, Lemma 3.1] that, again for polynomial mortar spaces, Π_0 could be defined in the case we consider in this paper of two grid sizes, h for the subdomains, and H for the interface. However, we have changed the definition of the mortar space M_H, and thus also the definition of $\mathbf{V}_{h,0}$ and Π_0. Since the proof of this lemma changes little from [6, section 3] and is rather technical, we delay it to Appendix B.

4.2. Mortar homogenization approximation. Before turning to the proof of the error estimates, we prove a lemma regarding mortar approximation, as alluded to in (3.6) above when motivating the definition of M_H. We give two versions of the approximation, depending on whether the homogenization-based mortar space has a generating polynomial space of degree rich enough to contain a C^1 subspace of approximation order $\mathcal{O}(H^m)$ over Γ. In that case, let $\mathcal{I}_H^c$ be the interpolation or H^2 projection operator into this C^1 subspace. It has the approximation estimates

$$\|\psi - \mathcal{I}_H^c\psi\|_{\alpha,\Gamma} \le C\|\psi\|_{t,\Gamma}H^{t-\alpha}, \quad 0 \le t \le m, \quad 0 \le \alpha \le 2. \tag{4.17}$$

In the alternative case, we may simply let $\mathcal{I}_H^c$ be the piecewise interpolation or L^2 projection operator into the generating polynomial space, and note that

$$\|\psi - \mathcal{I}_H^c\psi\|_{0,\Gamma} \le C\|\psi\|_{t,\Gamma}H^t, \quad 0 \le t \le m, \tag{4.18}$$

$$\|\nabla_H(\psi - \mathcal{I}_H^c\psi)\|_{0,\Gamma} \le C\|\psi\|_{t,\Gamma}H^{t-1}, \quad 0 \le t \le m. \tag{4.19}$$

Finally, we define

$$\tilde{p} = \big(1 + \varepsilon\boldsymbol{\omega}(x, x/\varepsilon) \cdot \nabla_H\big)\mathcal{I}_H^c p_0, \tag{4.20}$$

wherein ∇_H may be replaced by ∇ in the smoother case.

LEMMA 4.3. *Suppose* $p_0 \in H^{m+1/2}(\Omega) \cap H^2(\Omega) \cap W^{1,\infty}(\Omega)$ *is the homogenized solution of* (3.8)–(3.10)*,* p *is the solution of* (1.1)–(1.5)*, and* $\tilde{p}$ *is defined by* (4.20)*. If* $\mathbf{v} \in \mathbf{V}_h$*, then for* $0 < t \leq m$*,*

$$\sum_{i=1}^{n} \big|\langle \tilde{p} - p, \mathbf{v}\cdot\nu\rangle_{\partial\Omega_i}\big| \leq C\big\{H^{t-1}(H+\varepsilon)(Lh)^{-1/2}\|p_0\|_{t+1/2} + \varepsilon\|p_0\|_2 + \sqrt{\varepsilon}\|\nabla p_0\|_{0,\infty}\big\}\|\mathbf{v}\|_{H(\mathrm{div})}. \tag{4.21}$$

Moreover, if the generating polynomial space contains a C^1 *subspace of approximation order* $\mathcal{O}(H^m)$ *over* Γ*, then*

$$\sum_{i=1}^{n} \big|\langle \tilde{p} - p, \mathbf{v}\cdot\nu\rangle_{\partial\Omega_i}\big| \leq C\big\{H^{t-3/2}(1+\varepsilon)L^{-1/2}\|p_0\|_{t+1/2} + \varepsilon\|p_0\|_2 + \sqrt{\varepsilon}\|\nabla p_0\|_{0,\infty}\big\}\|\mathbf{v}\|_{H(\mathrm{div})}. \tag{4.22}$$

Proof. Recall that $p_\varepsilon^1(x)$ is defined by (3.11). We first compute

$$\begin{aligned}
\big|\langle \tilde{p} - p, \mathbf{v}\cdot\nu\rangle_{\partial\Omega_i}\big| &= \big|\langle \tilde{p} - p_\varepsilon^1 + p_\varepsilon^1 - p, \mathbf{v}\cdot\nu\rangle_{\partial\Omega_i}\big| \\
&= \big|\langle(1 + \varepsilon\boldsymbol{\omega}(x, x/\varepsilon)\cdot\nabla_H)(\mathcal{I}_H^c p_0 - p_0) + (p_\varepsilon^1 - p), \mathbf{v}\cdot\nu\rangle_{\partial\Omega_i}\big| \\
&\leq \big|\langle(1 + \varepsilon\boldsymbol{\omega}(x, x/\varepsilon)\cdot\nabla_H)(\mathcal{I}_H^c p_0 - p_0), \mathbf{v}\cdot\nu\rangle_{\partial\Omega_i}\big| + \big|\langle p_\varepsilon^1 - p, \mathbf{v}\cdot\nu\rangle_{\partial\Omega_i}\big|.
\end{aligned} \tag{4.23}$$

The sum on i of the latter term is bounded using the first $H(\mathrm{div})$ trace theorem (4.12) and Lemma 3.1 as

$$\begin{aligned}
\sum_i \big|\langle p_\varepsilon^1 - p, \mathbf{v}\cdot\nu\rangle_{\partial\Omega_i}\big| &\leq \sum_i \|p_\varepsilon^1 - p\|_{1,\Omega_i}\|\mathbf{v}\|_{H(\mathrm{div};\Omega_i)} \leq \|p_\varepsilon^1 - p\|_1\|\mathbf{v}\|_{H(\mathrm{div})} \\
&\leq C\big\{\varepsilon\|p_0\|_2 + \sqrt{\varepsilon}\|\nabla p_0\|_{0,\infty}\big\}\|\mathbf{v}\|_{H(\mathrm{div})}.
\end{aligned} \tag{4.24}$$

For the other term, we use (4.18)–(4.19), the trace theorem (4.10), and the local inverse inequality (4.11) to compute

$$\begin{aligned}
&\big|\langle(1 + \varepsilon\boldsymbol{\omega}(x, x/\varepsilon)\cdot\nabla_H)(\mathcal{I}_H^c p_0 - p_0), \mathbf{v}\cdot\nu\rangle_{\partial\Omega_i}\big| \\
&\quad\leq \big\{\|\mathcal{I}_H^c p_0 - p_0\|_{0,\partial\Omega_i} + \varepsilon\|\boldsymbol{\omega}\|_{0,\infty}\|\nabla_H(\mathcal{I}_H^c p_0 - p_0)\|_{0,\partial\Omega_i}\big\}\|\mathbf{v}\cdot\nu\|_{0,\partial\Omega_i} \\
&\quad\leq C\|p_0\|_{t,\partial\Omega_i}H^{t-1}(H+\varepsilon)\|\mathbf{v}\cdot\nu\|_{0,\partial\Omega_i} \\
&\quad\leq C\|p_0\|_{t+1/2,\Omega_i}H^{t-1}(H+\varepsilon)\|\mathbf{v}\|_{0,\Omega_i}(Lh)^{-1/2}.
\end{aligned}$$

We obtain (4.21) from this and the previous two estimates (4.23)–(4.24). If instead we have the case of a smooth generating polynomial space, then we can argue using the second $H(\mathrm{div})$ trace theorem (4.13) as

$$\begin{aligned}
&\big|\langle(1 + \varepsilon\boldsymbol{\omega}(x, x/\varepsilon)\cdot\nabla)(\mathcal{I}_H^c p_0 - p_0), \mathbf{v}\cdot\nu\rangle_{\partial\Omega_i}\big| \\
&\quad\leq \|\mathcal{I}_H^c p_0 - p_0\|_{1/2,\partial\Omega_i}\|\mathbf{v}\|_{H(\mathrm{div};\Omega_i)} + \varepsilon\|\mathcal{I}_H^c p_0 - p_0\|_{3/2,\partial\Omega_i}\|\boldsymbol{\omega}\mathbf{v}\|_{H(\mathrm{div};\Omega_i)} \\
&\quad\leq \|\mathcal{I}_H^c p_0 - p_0\|_{1/2,\partial\Omega_i}\|\mathbf{v}\|_{H(\mathrm{div};\Omega_i)} \\
&\qquad + \|\mathcal{I}_H^c p_0 - p_0\|_{3/2,\partial\Omega_i}\big[\varepsilon\|\boldsymbol{\omega}\|_{0,\infty,\Omega_i}\|\mathbf{v}\|_{H(\mathrm{div};\Omega_i)} + \|\boldsymbol{\omega}\|_{1,\infty,\Omega_i}\|\mathbf{v}\|_{0,\Omega_i}\big] \\
&\quad\leq C\|p_0\|_{t+1/2,\Omega_i}H^{t-3/2}(H+\varepsilon+1)L^{-1/2}\|\mathbf{v}\|_{H(\mathrm{div};\Omega_i)},
\end{aligned}$$

and obtain (4.22). ∎

4.3. Proof of the velocity error estimates. We now prove the velocity bounds of (4.6)–(4.9) of Theorem 4.1. Using properties of the projection operators $\hat{\cdot}$ and Π_0, the equations for the error (3.4)–(3.5) become

$$(a_\varepsilon^{-1}(\mathbf{u}-\mathbf{u}_h),\mathbf{v}) - \sum_{i=1}^n \left[(\hat{p}-p_h,\nabla\cdot\mathbf{v})_{\Omega_i} - \langle p,\mathbf{v}\cdot\nu_i\rangle_{\Gamma_i}\right] = 0 \quad \forall\,\mathbf{v}\in\mathbf{V}_{h,0}, \tag{4.25}$$

$$\sum_{i=1}^n(\nabla\cdot(\Pi_0\mathbf{u}-\mathbf{u}_h),w)_{\Omega_i} = 0 \quad \forall\, w\in W_h. \tag{4.26}$$

Note that the latter equation implies that

$$\nabla\cdot(\Pi_0\mathbf{u}-\mathbf{u}_h) = 0. \tag{4.27}$$

Taking $\mathbf{v} = \Pi_0\mathbf{u}-\mathbf{u}_h \in \mathbf{V}_{h,0}$ in (4.25), we have

$$\begin{aligned}(a_\varepsilon^{-1}(\mathbf{u}-\mathbf{u}_h),\Pi_0\mathbf{u}-\mathbf{u}_h) &= -\sum_{i=1}^n\langle p,(\Pi_0\mathbf{u}-\mathbf{u}_h)\cdot\nu_i\rangle_{\Gamma_i}\\ &= \sum_{i=1}^n\langle \tilde{p}-p,(\Pi_0\mathbf{u}-\mathbf{u}_h)\cdot\nu_i\rangle_{\Gamma_i},\end{aligned} \tag{4.28}$$

where $\tilde{p}\in M_H$ is defined by (4.20). Now

$$\begin{aligned}\|\mathbf{u}-\mathbf{u}_h\|_0^2 &\le C\big\{(a_\varepsilon^{-1}(\mathbf{u}-\mathbf{u}_h),\Pi_0\mathbf{u}-\mathbf{u}_h) + (a_\varepsilon^{-1}(\mathbf{u}-\mathbf{u}_h),\mathbf{u}-\Pi_0\mathbf{u})\big\}\\ &\le C\big\{(a_\varepsilon^{-1}(\mathbf{u}-\mathbf{u}_h),\Pi_0\mathbf{u}-\mathbf{u}_h) + \|\mathbf{u}-\Pi_0\mathbf{u}\|^2\big\} + \tfrac{1}{2}\|\mathbf{u}-\mathbf{u}_h\|^2,\end{aligned}$$

and so with (4.28), we are lead to the estimate

$$\begin{aligned}\|\Pi_0\mathbf{u}-\mathbf{u}_h\|_0^2 &\le C\big\{\|\Pi_0\mathbf{u}-\mathbf{u}\|_0^2 + \big|(a_\varepsilon^{-1}(\mathbf{u}-\mathbf{u}_h),\Pi_0\mathbf{u}-\mathbf{u}_h)\big|\big\}\\ &\le C\left\{\|\Pi_0\mathbf{u}-\mathbf{u}\|_0^2 + \sum_{i=1}^n\left|\langle\tilde{p}-p,(\Pi_0\mathbf{u}-\mathbf{u}_h)\cdot\nu_i\rangle_{\partial\Omega_i}\right|\right\}\\ &\le C\big\{E_{\mathrm{L}4.2}^2 + \tilde{E}_{\mathrm{L}4.3}\|\Pi_0\mathbf{u}-\mathbf{u}_h\|_0\big\},\end{aligned} \tag{4.29}$$

where $E_{\mathrm{L}4.2}$ is the bound on $\|\Pi_0\mathbf{u}-\mathbf{u}\|_0$ from either (4.15) or (4.16) of Lemma 4.2, and where $\tilde{E}_{\mathrm{L}4.3}$ is the main factor of the bound on the mortar approximation from either (4.21) or (4.22) of Lemma 4.3. The four velocity error estimates (4.6)–(4.9) of Theorem 4.1 follow.

4.4. Proof of the pressure error estimates. We now prove the pressure error bounds of (4.6)–(4.9). Let ϕ be the solution of

$$\begin{aligned}\Delta\phi &= \hat{p}-p_h \quad &&\text{in } \Omega,\\ \phi &= 0 &&\text{on } \partial\Omega,\end{aligned}$$

which, by elliptic regularity, satisfies

$$\|\phi\|_2 \le C\|\hat{p}-p_h\|_0. \tag{4.30}$$

Now

$$\|\hat{p}-p_h\|_0^2 = (\hat{p}-p_h,\Delta\phi) = (\hat{p}-p_h,\nabla\cdot\Pi_0\nabla\phi), \tag{4.31}$$

and taking $\mathbf{v} = \Pi_0 \nabla\phi$ in (4.25) and using weak continuity of $\mathbf{v} \in \mathbf{V}_{h,0}$, we have

$$\|\hat{p} - p_h\|_0^2 = (a_\varepsilon^{-1}(\mathbf{u} - \mathbf{u}_h), \Pi_0\nabla\phi) + \sum_{i=1}^{n} \langle p - \tilde{p}, \Pi_0\nabla\phi \cdot \nu_i\rangle_{\Gamma_i}, \tag{4.32}$$

where $\tilde{p} \in M_H$ is again defined by (4.20). We obtain

$$\|\hat{p} - p_h\|_0^2 \le C\big\{\|\mathbf{u} - \mathbf{u}_h\|_0 + \tilde{E}_{\mathrm{L4.3}}\big\}\|\Pi_0\nabla\phi\|_{H(\mathrm{div})},$$

where $\tilde{E}_{\mathrm{L4.3}}$ is the error factor from Lemma 4.3, which depends on whether we use (4.21) or (4.22). Since $\nabla \cdot \Pi_0\nabla\phi = \hat{p} - p_h$ and, using (4.16) and (4.30),

$$\|\Pi_0\nabla\phi\|_0 \le \|\Pi_0\nabla\phi - \nabla\phi\|_0 + \|\nabla\phi\|_0 \le C\big((hH/L)^{1/2} + 1\big)\|\phi\|_2 \le C\|\hat{p} - p_h\|_0,$$

we have that

$$\|\Pi_0\nabla\phi\|_{H(\mathrm{div})} \le C\|\hat{p} - p_h\|_0,$$

and the proof of Theorem 4.1 is complete.

5. Numerical results. In this section we present some numerical results that show the value in using the homogenization-based mortar space as opposed to using simple polynomial mortar spaces. Our theoretical results show that the method works well in the case when a_ε has a two-scale structure (3.7). Thus our objective for the numerical tests is to consider the performance of the method when applied to problems that do *not* obviously possess this two-scale structure.

In all our examples, we use a two-dimensional rectangular domain broken into a rectangular array of subdomains Ω_i, each of which has a rectangular fine grid. The subdomain problems are approximated using the lowest order Raviart–Thomas spaces RT0 [33] for $\mathbf{V}_{h,i} \times W_{h,i}$, which have $k = \ell = 1$. For the mortar grid, we take a single element along each interface $\Gamma_{ij} = \bar{\Omega}_i \cap \bar{\Omega}_j$. We contrast the use of discontinuous polynomial mortar spaces M_H of degree 1 (P1M, linears with $m = 2$ degrees of freedom per mortar edge) and degree 2 (P2M, quadratics with $m = 3$ degrees of freedom per mortar edge) with the homogenization-based multiscale mortar space (MSM) with a discontinuous generating polynomial space of degree 1 (for which $m = 2$). However, we note that formally in terms of polynomial approximation, the space MSM contains only polynomials of degree 0, for which $m = 1$. Recall that in subsection 3.2, we noted that this MSM mortar space has three degrees of freedom per mortar edge, so the fair comparison is with the quadratic mortar P2M.

A practical question arises: How do we define the mortar space, and in particular $\varepsilon\omega_k(x, x/\varepsilon)$? We use an approach described in [3]. For each interface Γ_{ij}, we define $\omega_{\Gamma_{ij},k}(x)$ as the periodic solution to

$$-\nabla \cdot \big[a_\varepsilon\big(\nabla\omega_{\Gamma_{ij},k} + \mathbf{e}_k\big)\big] = 0 \quad \text{in } \Omega_i \cup \Omega_j \cup \Gamma_{ij}, \tag{5.1}$$

and then in the definition (3.14) of M_h,

$$(1 + \varepsilon\boldsymbol{\omega}(x, x/\varepsilon) \cdot \nabla_H) \quad \text{is replaced by} \quad (1 + \boldsymbol{\omega}_{\Gamma_{ij}}(x) \cdot \nabla_H) \quad \text{for } x \in \Gamma_{ij}, \tag{5.2}$$

where $\boldsymbol{\omega}_{\Gamma_{ij}} = (\omega_{\Gamma_{ij},1}, \dots, \omega_{\Gamma_{ij},d})^T$. Note that the domain $\Omega_i \cup \Omega_j \cup \Gamma_{ij}$ is not scaled to unit size, so scaling by ε is not needed in the second expression. Hou and Wu [21] introduced an oversampling technique that better captures the microstructure when defining multiscale finite elements. We can use the same idea here in the definition of the homogenization functions ω_k; that is, we can solve (5.1) on a domain larger than $\Omega_i \cup \Omega_j \cup \Gamma_{ij}$. In our numerical results, the oversampled version of the homogenization-based multiscale mortar space (MSM-OS) in two dimensions uses the six subdomains that surround Γ_{ij} (or fewer, if we are near $\partial\Omega$). This reduces errors associated with the ends of Γ_{ij}. As a practical matter, we remark that the homogenization problems we compute are posed on domains larger than that of the subdomain problems; however, we could have reduced the size of the homogenization domain to one of comparable size, provided only that it contains Γ_{ij}.

In all our tests, the true solution is unknown, so we use as a reference the fine-scale RT0 solution.

5.1. A moderately heterogeneous permeability. The first numerical example is based on a moderately heterogeneous, mildly correlated, but locally isotropic permeability field $a_\varepsilon(x)$ that was geostatistically generated on a uniform 40×40 grid. It is depicted in Figure 5.1 on a log scale varying over about four orders of magnitude. The test is an example of a quarter five-spot pattern of wells, with an injection well in the lower left corner element and an extraction or production well in the upper right corner element. The domain is 40 meters square.

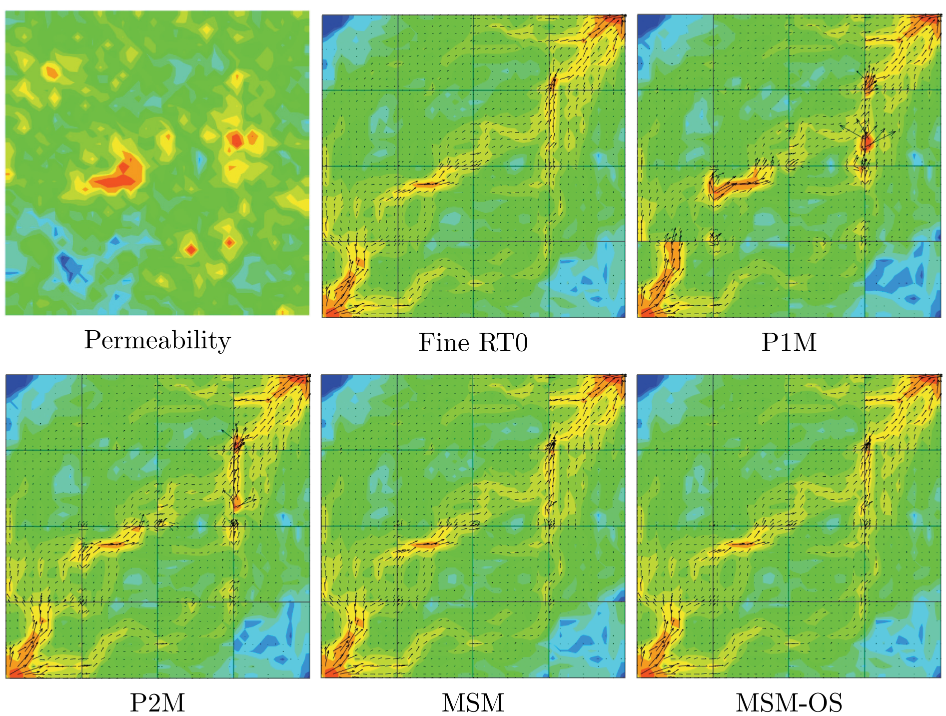

FIG. 5.1. *Moderate heterogeneity test. The fine permeability field is given on a* 40×40 *grid and depicted using a log scale varying from about* 0.32 *to* 3200 *millidarcy. The velocities are computed using RT*0 *on the fine grid and the mortar methods P*1*M, P*2*M, MSM, and MSM-OS, computed on the* 4×4 *coarse grid of subdomains with a* 10×10 *subgrid. The color depicts the speed, on a log scale from* 0.6 *to* 0.0006*, and the arrows show the velocity.*

In this test, we decompose the 40×40 fine grid into a 4×4 coarse grid of subdomains, each with a 10×10 subgrid. In Figure 5.1, we plot the speed $|\mathbf{u}|$ via color contours on a log scale, and also arrows representing the velocity vector $\mathbf{u}$

Table 5.1

Moderate heterogeneity test. Relative errors in the pressure and velocity for various mortar elements relative to the 40×40 *reference RT0 solution, using a* 4×4 *coarse grid (and* 10×10 *subgrid). Both* ℓ^2 *and* ℓ^∞ *(maximum) norm errors are shown.*

	Pressure error		Velocity error	
Method	ℓ^2	ℓ^∞	ℓ^2	ℓ^∞
P1M	0.1989	0.1452	0.4157	0.8042
P2M	0.0431	0.0353	0.2564	0.5267
MSM	0.0111	0.0137	0.1072	0.1432
MSM-OS	0.0088	0.0134	0.0822	0.1363

itself. We see visually that MSM and MSM-OS do a much better job of reproducing the fine-scale RT0 velocity than P1M and P2M. The visual evidence is corroborated quantitatively in Table 5.1, where we give the relative errors with respect to the fine RT0 solution computed in ℓ^2 and ℓ^∞.

The 8%–11% relative velocity errors in the ℓ^2-norm for MSM and MSM-OS are within reasonable engineering accuracy for subsurface flow problems, given the large uncertainty in the characterization of the permeability a_ε itself. Although formally both MSM (or MSM-OS) and P2M use the same number of degrees of freedom, the use of homogenization theory in the definition of M_H has clearly been of significant benefit, reducing the relative ℓ^2-velocity error from 26% to the 10% range.

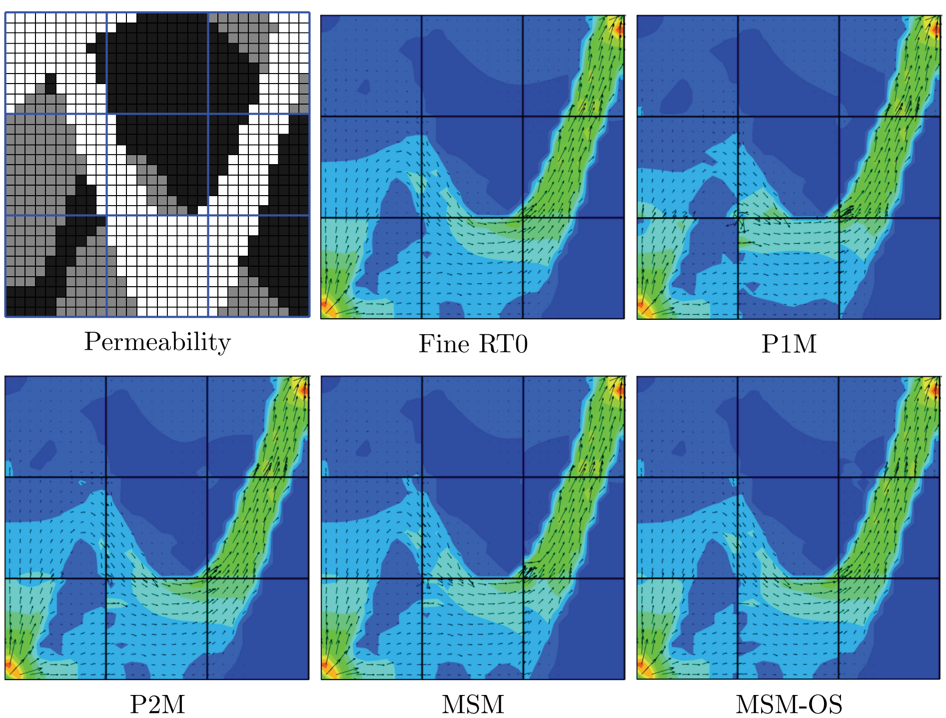

Fig. 5.2. *Simple channel test. The top left plot is the fine* 30×30 *grid permeability, which has only three values:* 10 *(white),* 1 *(gray), and* 0.1 *(black) darcy. The RT0 solution uses the fine* 30×30 *grid. Mortar results use a coarse* 3×3 *grid of subdomains with a* 10×10 *subgrid. The color depicts the speed, on a log scale from* 0.55 *to* 0.0055*, and the arrows show the velocity.*

TABLE 5.2

Simple channel test. Relative errors in the pressure and velocity for the various mortar elements relative to the 30×30 *reference RT*0 *solution, using a* 3×3 *coarse grid (and* 10×10 *subgrid). Both* ℓ^2*- and* ℓ^∞*- (maximum) norm errors are shown.*

	Pressure error		Velocity error	
Method	ℓ^2	ℓ^∞	ℓ^2	ℓ^∞
P1M	0.0432	0.0168	0.1681	0.3603
P2M	0.0104	0.0033	0.0621	0.1762
MSM	0.0074	0.0021	0.1046	0.2891
MSM-OS	0.0087	0.0034	0.0671	0.1199

5.2. A simple channelized permeability. We next consider a relatively simple synthetic example taken from White and Horne [36]. The permeability, depicted in Figure 5.2, takes only three values on a fine 30×30 grid and exhibits a single fluvial channel of high permeability. This permeability clearly does not satisfy the two-scale separation hypothesis (3.7). We again consider a quarter five-spot pattern of wells, with wells in the lower left and upper right corners. The fine-scale RT0 solution clearly shows that fluid concentrates into the high permeability channel and tends to avoid the low permeability regions.

The mortar results in Figure 5.2 use a very coarse 3×3 grid of subdomains that clearly does not resolve the channel itself. Nevertheless, all of the mortar methods are able to resolve the flow within the channel. From Table 5.2, we quantify that P2M and MSM-OS do the best job at about 6%–7% ℓ^2-velocity error, although P1M and MSM are perhaps also reasonable at 17% and 10%, respectively.

5.3. A channelized permeability from SPE10. In our final test case, we take a permeability field from one layer of the Tenth Society of Petroleum Engineers Comparative Solution Project (SPE10) [13]. We take layer 85, which is shown in Figure 5.3. It is given on a fine 60×220 grid and varies over about seven orders of magnitude. We again simulate a quarter five-spot well pattern. The fine-scale RT0 solution shows that the permeability gives rise to strong, long-range channels and produces an extremely complex velocity field.

Our mortar results are computed over a coarse 3×11 grid of subdomains with a 20×20 subgrid and shown in Figure 5.3. At first glance, all methods appear to work relatively well. Careful examination reveals significant differences between the fine-scale RT0 result and P1M and P2M.

The relative errors are given in Table 5.3. The ℓ^2-velocity errors for MSM and MSM-OS mortars are in the reasonable range of 11%–16%, which is indeed much

TABLE 5.3

*SPE*10-85 *test. Relative errors in the pressure and velocity for the various mortar elements relative to the* 60×220 *reference RT*0 *solution, using a* 3×11 *coarse grid (and* 20×20 *subgrid). Both* ℓ^2*- and* ℓ^∞*- (maximum) norm errors are shown.*

	Pressure error		Velocity error	
Method	ℓ^2	ℓ^∞	ℓ^2	ℓ^∞
P1M	0.0642	0.0270	0.3985	0.7430
P2M	0.0359	0.0204	0.4058	0.9042
MSM	0.0100	0.0068	0.1599	0.3800
MSM-OS	0.0055	0.0031	0.1063	0.3180

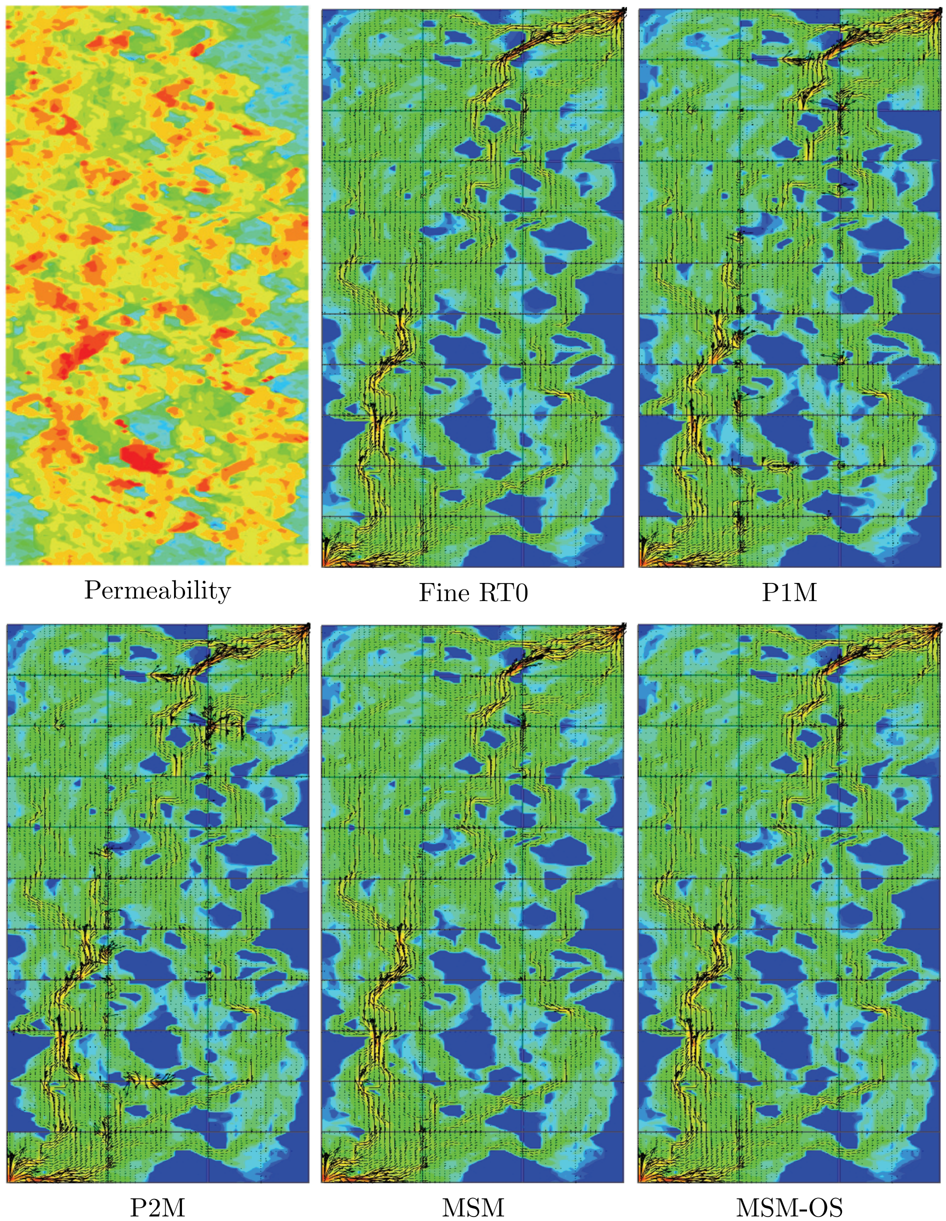

FIG. 5.3. *SPE10-85 test. The permeability field is on a* 60×220 *grid using a log scale from* 1.9e-11 *(red) to* 1.0e-18 *(blue)* m^2. *The fine-scale RT0 speed and velocity are plotted on a log scale from* 7.5e-6 *(red) to* 7.5e-9 *(blue). The mortar results come from a* 3×11 *coarse grid with a* 20×20 *subgrid using various mortar elements.*

better than P1M and P2M, which are about 40% in error. (Surprisingly, P1M is a little bit better than P2M for this example.)

6. Summary and concluding remarks. In a parallel computing environment, compared to the subdomain problems, the interface problem is much less efficiently solved. The multiscale mortar method [7] allows us to use fewer degrees of freedom for the interface problem, thereby increasing overall parallel efficiency. In the case where a_ε is nicely behaved (i.e., ε is not so small), a polynomial mortar space suffices to maintain accuracy.

Standard approximation estimates show that piecewise polynomial functions of degree $m-1$ formally approximate to order $\mathcal{O}(H^m)$, at the expense of requiring bounding m derivatives of the function being approximated. For a spatially heterogeneous problem, the solution's derivatives scale as ε^{-1}, and formal accuracy is lost when ε is small.

In the case that the permeability $a_\varepsilon(x)$ has two separated scales (3.7), we have a theoretical result from homogenization theory that relates the solution to the microstructure. Based on this approximation, $p \approx p_\varepsilon^1$ from Lemma 3.1, we defined a new mortar space M_H using polynomial generating spaces of degree $m-1$. We proved in Lemma 4.3 that the new mortar approximation of p on the interface achieves essentially the formal accuracy $\mathcal{O}(H^m)$, but requires bounds only on derivatives of p_0, the coarse-scale homogenized solution, up to a factor $\mathcal{O}(\sqrt{\varepsilon})$. This led to Theorem 4.1, where we proved optimal order error estimates in the discretization parameters and good approximation when ε is small.

In the highly heterogeneous case that $a_\varepsilon(x)$ does *not* have two separated scales but ε is small, our new mortar space can still be defined. We showed by numerical examples that the new mortar space performs better than purely polynomial-based mortar spaces. That is, our mortar coupling spaces have only a few degrees of freedom per subdomain interface, and the new homogenization-based mortar approach makes better use of them in terms of multiscale approximation, leading to a more efficient domain decomposition method in parallel.

Appendix A. An example satisfying Assumption 4.1. In this appendix, we show that Assumption 4.1 is satisfied by a two-dimensional example based on using RT0 spaces over the subdomains. We make the following technical assumption.

Assumption A.1. For $\mu \in M_H$, the condition

$$\mathcal{Q}_{h,i}\mu = 0, \quad i = 1,\dots,n, \quad \text{implies that } \mu = 0. \tag{A.1}$$

This assumption is necessary for unique solvability of the method, as noted at the end of section 2.1. It is also reasonable, first because our mortar space has just a few degrees of freedom compared to the traces of the discrete normal velocities, and second because it is easy to verify in practice (after refining the fine grid if necessary).

Providing conditions for the establishment of Assumption 4.1, which requires uniformity in h, H, L, and ε, is especially difficult because the local basis for M_H may degenerate. To overcome this difficulty, we make another technical assumption.

Assumption A.2. There exists C, independent of h, H, L, and ε, such that for any $\mu \in M_{H,ij}$, the derivative μ' satisfies

$$\|\mu'\|_{0,\Gamma_{ij}} \le C\varepsilon^{-1}\|\mu\|_{0,\Gamma_{ij}}. \tag{A.2}$$

This bound can be justified as follows. Recall that on a single mortar element $e \in \mathcal{T}_{H,ij}$, $M_{H,e}$ is three dimensional, as noted at the end of section 3.2. For convenience, we use the notation given there (so, e.g., x is the variable along the interface), and recall the basis

$$\big\{1,\ \varphi_1^\varepsilon(x) \equiv x + \varepsilon\omega_1\big((x,0),(x,0)/\varepsilon\big), \varphi_2^\varepsilon(x) \equiv \omega_2\big((x,0),(x,0)/\varepsilon\big)\big\}.$$

Since $\|\mu'\|_{0,\Gamma_{ij}}$ is a seminorm on the space, we have the desired bound

$$\|\mu'\|_{0,\Gamma_{ij}} \le C_\varepsilon \|\mu\|_{0,\Gamma_{ij}}, \tag{A.3}$$

except that C_ε will depend on ε.

We believe that C_ε scales as ε^{-1}, because the arguments of the functions in $M_{H,e}$ scale this way. However, it is difficult to establish this result as $\varepsilon \to 0$. In the limit, $\varphi_1^\varepsilon \to x$ is fine, but $\varphi_2^\varepsilon(x) = \omega_2$ tends weakly to its average, which may be constant over some edge Γ_{ij}, and so the space $M_{H,ij}$ would degenerate to two dimensions.

However, it makes little sense to allow ε to tend to zero, since we have assumed that the heterogeneity can be resolved by finite $h < \varepsilon$. If we assume a lower cut-off on the scales, say, $\varepsilon \ge \varepsilon_* > 0$, then we avoid any potential degeneracy. Moreover, since our spaces M_H depend continuously on ε, we can conclude that C_ε in (A.3) is also a continuous function of ε on the compact interval $[\varepsilon_*, 1]$. Thus C_ε has a maximum, and we obtain Assumption A.2, in fact, with the bound (A.2) independent of ε (but depending now on ε_*).

LEMMA A.1. *If two-dimensional* $RT0$ *spaces are used to approximate the subdomain problems, the interface grid matches with the subdomain grid, and Assumptions* A.1–A.2 *hold, then there exists* $0 < \gamma \le 1$ *such that Assumption* 4.1 *holds provided that* $h \le \gamma\varepsilon$. *That is, there exists* C *and* $\gamma > 0$, *independent of* h, H, L, *and* ε, *such that for any* $h \le \gamma\varepsilon$, $\mu \in M_H$, *and* Γ_{ij},

$$\|\mu\|_{0,\Gamma_{ij}} \le C\big\{\|\mathcal{Q}_{h,i}\mu\|_{0,\Gamma_{ij}} + \|\mathcal{Q}_{h,j}\mu\|_{0,\Gamma_{ij}}\big\}. \tag{A.4}$$

Proof. By Assumption A.1, $\|\mathcal{Q}_{h,i}\mu\|_{0,\Gamma_{ij}} + \|\mathcal{Q}_{h,j}\mu\|_{0,\Gamma_{ij}}$ is a norm on the finite-dimensional space $M_{H,ij}$. Thus, there is a constant $C_{H,h,\varepsilon}$ satisfying (A.4). Because the coarse interface grid matches the fine subdomain grids, a standard scaling argument can be given to show that $C_{H,h,\varepsilon}$ is independent of H. Henceforth, without loss of generality, we shall assume that Γ_{ij} consists of a single element of unit size, so Γ_{ij} becomes $(0,1)$. It remains to show that $C_{H,h,\varepsilon} = C_{h,\varepsilon}$ is independent of h and ε.

Restrict to one side (call it ℓ) of the interface and simply let $\mathcal{Q}_h = \mathcal{Q}_{h,\ell}$. For RT0, $\mathcal{Q}_h\mu$ is just the average of μ on each fine-scale element. Using Assumption A.2 and a standard approximation result, we compute

$$\begin{aligned}
\|\mu\|_{0,(0,1)} &\le \|Q_h\mu\|_{0,(0,1)} + \|\mu - Q_h\mu\|_{0,(0,1)} \\
&\le \|Q_h\mu\|_{0,(0,1)} + C\|\mu'\|_{0,(0,1)}h \\
&\le \|Q_h\mu\|_{0,(0,1)} + C^*\|\mu\|_{0,(0,1)}h/\varepsilon,
\end{aligned}$$

where C and C^* are independent of our parameters. Thus if $\gamma = 1/(2C^*)$ and $h \le \gamma\varepsilon$, we obtain our bound and the proof is complete. ∎

Appendix B. A Proof of the existence of Π_0. In this appendix, we give a proof of Lemma 4.2, following closely the proof given in [6, section 3], which makes strong use of double-valued functions on Γ. For each $i = 1, \dots, n$, let the normal traces of the velocities be

$$\Lambda_{h,i} = \mathbf{V}_{h,i} \cdot \nu_i|_{\partial\Omega_i},$$

and recall that we defined the interface L^2 projection operator $\mathcal{Q}_{h,i} : L^2(\partial\Omega_i) \to \Lambda_{h,i}$ such that, for all $\phi \in L^2(\partial\Omega_i)$,

$$\langle \phi - \mathcal{Q}_{h,i}\phi, \xi\rangle_{\partial\Omega_i} = 0 \quad \forall \xi \in \Lambda_{h,i}.$$

Clearly,

$$\|\phi - \mathcal{Q}_{h,i}\phi\|_{-\alpha,\Gamma_{ij}} \le C\|\phi\|_{r,\Gamma_{ij}} h^{r+\alpha}, \quad 0 \le r \le k, \quad 0 \le \alpha \le k. \tag{B.1}$$

Next we define the traces of weakly continuous velocities as

$$\begin{aligned}\mathbf{\Lambda}_{h,0} = \big\{ &\boldsymbol{\phi} \in (L^2(\Gamma))^2 : \forall i < j,\\ &\boldsymbol{\phi}|_{\Gamma_{ij}} = (\phi_i, \phi_j) = (\mathbf{v}\cdot\nu_i, \mathbf{v}\cdot\nu_j) \text{ for some } \mathbf{v} \in \mathbf{V}_{h,0}\big\},\end{aligned}$$

with the indexing convention that $\boldsymbol{\phi}|_{\Gamma_{ij}} = (\phi_i, \phi_j)$ for $i < j$. For this space, we define the $(L^2)^2$ projection operator $\boldsymbol{\mathcal{Q}}_{h,0} : (L^2(\Gamma))^2 \to \mathbf{\Lambda}_{h,0}$ by

$$\sum_{i=1}^{n} \langle \phi_i - (\boldsymbol{\mathcal{Q}}_{h,0}\boldsymbol{\phi})_i, \xi_i \rangle_{\Gamma_i} = 0 \quad \forall \boldsymbol{\xi} \in \mathbf{\Lambda}_{h,0}.$$

By the definition of weakly continuous velocities (3.1), we note that

$$\langle (\boldsymbol{\mathcal{Q}}_{h,0}\boldsymbol{\phi})_i + (\boldsymbol{\mathcal{Q}}_{h,0}\boldsymbol{\phi})_j, \mu \rangle_{\Gamma_{ij}} = 0 \quad \forall \mu \in M_{H,ij}. \tag{B.2}$$

Our projection Π_0 is a modification of the standard Fortin projection [33, 11, 34]. Let $\Pi_i : (H^\eta(\Omega_i))^d \cap H(\text{div};\Omega_i) \to \mathbf{V}_{h,i}$ be this standard projection operator, and recall that the L^2 projection of $\phi \in L^2$ into W_h is denoted as $\hat{\phi} \in W_h$. These projections have the properties that

$$\nabla\cdot\Pi_i\mathbf{v} = \widehat{\nabla\cdot\mathbf{v}}\big|_{\Omega_i}, \tag{B.3}$$

$$(\Pi_i\mathbf{v})\cdot\nu_i = \mathcal{Q}_{h,i}(\mathbf{v}\cdot\nu_i), \tag{B.4}$$

$$\|\mathbf{v} - \Pi_i\mathbf{v}\|_{0,\Omega_i} \le C\|\mathbf{v}\|_{r,\Omega_i} h^r, \quad 0 < r \le k, \tag{B.5}$$

where the latter estimate for $0 < r < 1$ is due to Mathew [26] and Arbogast et al. [6]. Our projection Π_0 is simply

$$\Pi_0\mathbf{v}|_{\Omega_i} = \Pi_i(\mathbf{v} + \boldsymbol{\psi}_i), \tag{B.6}$$

where $\boldsymbol{\psi}_i = \nabla\theta_i$ is defined to adjust the boundary. To this end, for $\mathbf{v} \in H(\text{div})$, we consider $\mathbf{v}\cdot\nu \in (L^2(\Gamma))^2$, where

$$\mathbf{v}\cdot\nu|_{\Gamma_{ij}} = (\mathbf{v}\cdot\nu_i, \mathbf{v}\cdot\nu_j),$$

and then we require that

$$\Delta\theta_i = \nabla\cdot\boldsymbol{\psi}_i = 0 \qquad \text{in } \Omega_i, \tag{B.7}$$

$$\nabla\theta_i\cdot\nu_i = \boldsymbol{\psi}_i\cdot\nu_i = (\boldsymbol{\mathcal{Q}}_{h,0}\mathbf{v}\cdot\nu)_i - \mathcal{Q}_{h,i}\mathbf{v}\cdot\nu_i \quad \text{on } \partial\Omega_i. \tag{B.8}$$

These elliptic problems are well defined, since we assume that M_H and $\Lambda_{h,i}$ contain piecewise constant functions defined over each Γ_{ij}. Note that Π_0 maps into the weakly continuous space $\mathbf{V}_{h,0}$ as required, since for any $\mu \in M_H$,

$$\begin{aligned}\langle \Pi_0\mathbf{v}\cdot\nu_i + \Pi_0\mathbf{v}\cdot\nu_j, \mu\rangle_{\Gamma_{ij}} &= \langle \Pi_i(\mathbf{v}+\boldsymbol{\psi}_i)\cdot\nu_i + \Pi_j(\mathbf{v}+\boldsymbol{\psi}_j)\cdot\nu_j, \mu\rangle_{\Gamma_{ij}}\\ &= \langle (\boldsymbol{\mathcal{Q}}_{h,0}\mathbf{v}\cdot\nu)_i + (\boldsymbol{\mathcal{Q}}_{h,0}\mathbf{v}\cdot\nu)_j, \mu\rangle_{\Gamma_{ij}} = 0,\end{aligned}$$

by (B.8), (B.4), and (B.2). Moreover, the divergence is preserved by (B.3) and (B.7), i.e., (4.14) holds. We have the standard energy and elliptic regularity estimates (assuming that each Ω_i has a reasonable boundary; see [20, 17]),

$$\|\boldsymbol{\psi}_i\|_{0,\Omega_i} \le C\|(\boldsymbol{\mathcal{Q}}_{h,0}\mathbf{v}\cdot\nu)_i - \mathcal{Q}_{h,i}\mathbf{v}\cdot\nu_i\|_{-1/2,\partial\Omega_i},$$
$$\|\boldsymbol{\psi}_i\|_{1/2,\Omega_i} \le C\|(\boldsymbol{\mathcal{Q}}_{h,0}\mathbf{v}\cdot\nu)_i - \mathcal{Q}_{h,i}\mathbf{v}\cdot\nu_i\|_{0,\partial\Omega_i},$$

where C is independent of L, which can be seen by scaling the domain in (B.7)–(B.8) to unit size so that the boundary term becomes $L[(\boldsymbol{\mathcal{Q}}_{h,0}\mathbf{v}\cdot\nu)_i - \mathcal{Q}_{h,i}\mathbf{v}\cdot\nu_i]$.

It remains to prove the approximation estimates (4.15)–(4.16). By (B.5), we need only estimate $\|\Pi_i\boldsymbol{\psi}_i\|_{0,\Omega_i}$. To this end, we note that

$$\begin{aligned}\|\Pi_i\boldsymbol{\psi}_i\|_{0,\Omega_i} &\le \|\Pi_i\boldsymbol{\psi}_i - \boldsymbol{\psi}_i\|_{0,\Omega_i} + \|\boldsymbol{\psi}_i\|_{0,\Omega_i} \le Ch^{1/2}\|\boldsymbol{\psi}_i\|_{1/2,\Omega_i} + \|\boldsymbol{\psi}_i\|_{0,\Omega_i}\\ &\le C\big\{h^{1/2}\|(\boldsymbol{\mathcal{Q}}_{h,0}\mathbf{v}\cdot\nu)_i - \mathcal{Q}_{h,i}\mathbf{v}\cdot\nu_i\|_{0,\partial\Omega_i} + \|(\boldsymbol{\mathcal{Q}}_{h,0}\mathbf{v}\cdot\nu)_i - \mathcal{Q}_{h,i}\mathbf{v}\cdot\nu_i\|_{-1/2,\partial\Omega_i}\big\}.\end{aligned}$$

The following lemma can be used with the trace theorem (4.10) to complete the proof of Lemma 4.2.

LEMMA B.1. *If Assumption* 4.1 *holds, then there is a constant C, independent of h, H, L, and ε, such that for any $\mathbf{v}\in H^{r+1/2}(\Omega)$, $0\le r\le k$, and $0\le\alpha\le 1$,*

$$\left\{\sum_{i=1}^{n}\|(\boldsymbol{\mathcal{Q}}_{h,0}\mathbf{v}\cdot\nu)_i - \mathcal{Q}_{h,i}\mathbf{v}\cdot\nu_i\|^2_{-\alpha,\partial\Omega_i}\right\}^{1/2} \le C\|\mathbf{v}\|_{r,\Gamma}h^r(H+\varepsilon)^\alpha. \tag{B.9}$$

To prove (B.9), we need the following critical but very general lift property of mortar spaces; it and its proof can be found in [6, Lemma 3.1]. Recall that Assumption A.1 is implied by Assumption 4.1.

LEMMA B.2. *Suppose Assumption A.*1 *holds and M_H contains piecewise constant functions defined over the Γ_{ij}. For any $\boldsymbol{\phi}\in(L^2(\Gamma))^2$, extended by zero to $\partial\Omega$ and indexed by i and j on Γ_{ij}, there exists $\mu_H\in M_H$ such that on each Γ_{ij},*

$$\mathcal{Q}_{h,i}\mu_H = \mathcal{Q}_{h,i}\phi_i - (\boldsymbol{\mathcal{Q}}_{h,0}\boldsymbol{\phi})_i,$$
$$\mathcal{Q}_{h,j}\mu_H = \mathcal{Q}_{h,j}\phi_j - (\boldsymbol{\mathcal{Q}}_{h,0}\boldsymbol{\phi})_j,$$
$$\langle\mu_H,1\rangle_{\Gamma_{ij}} = \langle\mathcal{Q}_{h,i}\mu_H,1\rangle_{\Gamma_{ij}} = \tfrac12\langle\phi_i+\phi_j,1\rangle_{\Gamma_{ij}}.$$

Proof of Lemma B.1. Applying Lemma B.2 to $\mathbf{v}\cdot\nu$ gives $\mu_H\in M_H$ such that

$$\mathcal{Q}_{h,i}\mu_H = (\boldsymbol{\mathcal{Q}}_{h,0}\mathbf{v}\cdot\nu)_i - \mathcal{Q}_{h,i}\mathbf{v}\cdot\nu_i \quad\text{and}\quad \langle\mu_H,1\rangle_{\Gamma_{ij}} = \langle\mathcal{Q}_{h,i}\mu_H,1\rangle_{\Gamma_{ij}} = 0,$$

and so, using (B.2), the fact that $\mathbf{v}\cdot\nu_i + \mathbf{v}\cdot\nu_j = 0$ on Γ_{ij}, and Assumption 4.1,

$$\begin{aligned}\sum_i\|(\boldsymbol{\mathcal{Q}}_{h,0}\mathbf{v}\cdot\nu)_i - \mathcal{Q}_{h,i}\mathbf{v}\cdot\nu_i\|^2_{0,\Gamma_i} &= \sum_i\|\mathcal{Q}_{h,i}\mu_H\|^2_{0,\Gamma_i} = \sum_i\langle\mathcal{Q}_{h,i}\mu_H,\mu_H\rangle_{\Gamma_i}\\ &= \sum_i\langle(\boldsymbol{\mathcal{Q}}_{h,0}\mathbf{v}\cdot\nu)_i - \mathcal{Q}_{h,i}\mathbf{v}\cdot\nu_i,\mu_H\rangle_{\Gamma_i} = \sum_i\langle(1-\mathcal{Q}_{h,i})\mathbf{v}\cdot\nu_i,\mu_H\rangle_{\Gamma_i}\\ &\le \sum_i\|(1-\mathcal{Q}_{h,i})\mathbf{v}\cdot\nu_i\|_{0,\Gamma_i}\|\mu_H\|_{0,\Gamma_i}\\ &\le \tfrac12\sum_i\|(1-\mathcal{Q}_{h,i})\mathbf{v}\cdot\nu_i\|^2_{0,\Gamma_i} + \tfrac12\sum_i\|\mathcal{Q}_{h,i}\mu_H\|^2_{0,\Gamma_i},\end{aligned}$$

and (B.1) gives the $\alpha=0$ case of Lemma B.1.

For the case $\alpha = 1$, let $\rho \in H^1(\Gamma_{ij})$ and define ρ_{ij} as its $H^1(\Gamma_{ij})$ projection into the generating polynomial space for $M_{H,ij}$. With

$$\tilde{\rho}_{ij} = \big(1 + \varepsilon \boldsymbol{\omega}(x, x/\varepsilon) \cdot \nabla_H\big)\rho_{ij} \in M_{H,ij}, \tag{B.10}$$

we have that

$$\|\rho - \tilde{\rho}_{ij}\|_{0,\Gamma_{ij}} \le \|\rho - \rho_{ij}\|_{0,\Gamma_{ij}} + \varepsilon\|\boldsymbol{\omega}\|_{0,\infty}\|\nabla_H \rho_{ij}\|_{0,\Gamma_{ij}} \le C(H+\varepsilon)\|\rho\|_{1,\Gamma_{ij}}. \tag{B.11}$$

Now

$$\begin{aligned}
\langle(\boldsymbol{\mathcal{Q}}_{h,0}\mathbf{v}\cdot\nu)_i - \mathcal{Q}_{h,i}\mathbf{v}\cdot\nu_i, \rho\rangle_{\Gamma_{ij}} &= \langle \mathcal{Q}_{h,i}\mu_H, \rho\rangle_{\Gamma_{ij}} = \langle \mu_H, \mathcal{Q}_{h,i}\rho\rangle_{\Gamma_{ij}} \\
&= \tfrac{1}{2}\langle \mu_H, (\mathcal{Q}_{h,i} - \mathcal{Q}_{h,j})\rho\rangle_{\Gamma_{ij}} + \tfrac{1}{2}\langle \mu_H, (\mathcal{Q}_{h,i} + \mathcal{Q}_{h,j})\rho\rangle_{\Gamma_{ij}} \\
&\le C\|\mu_H\|_{0,\Gamma_{ij}} h\|\rho\|_{1,\Gamma_{ij}} + \tfrac{1}{2}\langle \mu_H, (\mathcal{Q}_{h,i} + \mathcal{Q}_{h,j})\rho\rangle_{\Gamma_{ij}},
\end{aligned}$$

using (B.1), and

$$\begin{aligned}
\langle \mu_H, (\mathcal{Q}_{h,i} + \mathcal{Q}_{h,j})\rho\rangle_{\Gamma_{ij}} &= \langle (\mathcal{Q}_{h,i} + \mathcal{Q}_{h,j})\mu_H, \rho\rangle_{\Gamma_{ij}} \\
&= \langle [(\boldsymbol{\mathcal{Q}}_{h,0}\mathbf{v}\cdot\nu)_i - \mathcal{Q}_{h,i}\mathbf{v}\cdot\nu_i] + [(\boldsymbol{\mathcal{Q}}_{h,0}\mathbf{v}\cdot\nu)_j - \mathcal{Q}_{h,j}\mathbf{v}\cdot\nu_j], \rho\rangle_{\Gamma_{ij}} \\
&= \langle (\boldsymbol{\mathcal{Q}}_{h,0}\mathbf{v}\cdot\nu)_i - \mathbf{v}\cdot\nu_i, \mathcal{Q}_{h,i}\rho\rangle_{\Gamma_{ij}} + \langle (\boldsymbol{\mathcal{Q}}_{h,0}\mathbf{v}\cdot\nu)_j - \mathbf{v}\cdot\nu_j, \mathcal{Q}_{h,j}\rho\rangle_{\Gamma_{ij}} \\
&= \langle (\boldsymbol{\mathcal{Q}}_{h,0}\mathbf{v}\cdot\nu)_i - \mathbf{v}\cdot\nu_i, \mathcal{Q}_{h,i}\rho - \tilde{\rho}_{ij}\rangle_{\Gamma_{ij}} + \langle (\boldsymbol{\mathcal{Q}}_{h,0}\mathbf{v}\cdot\nu)_j - \mathbf{v}\cdot\nu_j, \mathcal{Q}_{h,j}\rho - \tilde{\rho}_{ij}\rangle_{\Gamma_{ij}},
\end{aligned}$$

by (B.2) and the fact that $\mathbf{v}\cdot\nu_i + \mathbf{v}\cdot\nu_j = 0$. Thus, using (B.11) and (B.1),

$$\begin{aligned}
&\langle(\boldsymbol{\mathcal{Q}}_{h,0}\mathbf{v}\cdot\nu)_i - \mathcal{Q}_{h,i}\mathbf{v}\cdot\nu_i, \rho\rangle_{\Gamma_{ij}} \\
&\quad\le C\big\{\|\mu_H\|_{0,\Gamma_{ij}} h + \big[\|(\boldsymbol{\mathcal{Q}}_{h,0}\mathbf{v}\cdot\nu)_i - \mathbf{v}\cdot\nu_i\|_{0,\Gamma_{ij}} \\
&\qquad\qquad + \|(\boldsymbol{\mathcal{Q}}_{h,0}\mathbf{v}\cdot\nu)_j - \mathbf{v}\cdot\nu_j\|_{0,\Gamma_{ij}}\big](h + H + \varepsilon)\big\}\|\rho\|_{1,\Gamma_{ij}}.
\end{aligned}$$

Finally, a supremum on ρ combined with Assumption 4.1, the definition of μ_H, the already established $\alpha = 0$ case of this lemma, and (B.1) completes the proof of Lemma B.1, and therefore also Lemma 4.2. ∎

Remark B.1. If the polynomial generating space for $M_{H,ij}$ contains constant functions over the mesh $\mathcal{T}_{H,ij}$, then so does $M_{H,ij}$ itself. In that case, $\tilde{\rho}_{ij}$ in (B.10) may be defined using only these piecewise discontinuous constants, and ε does not appear in the estimate (B.9).

REFERENCES

[1] J. Aarnes and T. Y. Hou, *Multiscale domain decomposition methods for elliptic problems with high aspect ratios*, Acta Math. Appl. Sin. Engl. Ser., 18 (2002), pp. 63–76.

[2] J. E. Aarnes, Y. Efendiev, and L. Jiang, *Mixed multiscale finite element methods using limited global information*, Multiscale Model. Simul., 7 (2008), pp. 655–676.

[3] T. Arbogast, *Homogenization-based mixed multiscale finite elements for problems with anisotropy*, Multiscale Model. Simul., 9 (2011), pp. 624–653.

[4] T. Arbogast, *Mixed multiscale methods for heterogeneous elliptic problems*, in Numerical Analysis of Multiscale Problems, I. G. Graham et al., eds., Lect. Notes Comput. Sci. Eng. 83, Springer, Heidelberg, 2011, pp. 243–283.

[5] T. Arbogast and K. J. Boyd, *Subgrid upscaling and mixed multiscale finite elements*, SIAM J. Numer. Anal., 44 (2006), pp. 1150–1171.

[6] T. Arbogast, L. C. Cowsar, M. F. Wheeler, and I. Yotov, *Mixed finite element methods on nonmatching multiblock grids*, SIAM J. Numer. Anal., 37 (2000), pp. 1295–1315.

[7] T. Arbogast, G. Pencheva, M. F. Wheeler, and I. Yotov, *A multiscale mortar mixed finite element method*, Multiscale Model. Simul., 6 (2007), pp. 319–346.

[8] A. Bensoussan, J. L. Lions, and G. Papanicolaou, *Asymptotic Analysis for Periodic Structure*, North–Holland, Amsterdam, 1978.
[9] C. Bernardi, Y. Maday, and A. T. Patera, *A new nonconforming approach to domain decomposition: The mortar element method*, in Nonlinear Partial Differential Equations and Their Applications, H. Brezis and J. L. Lions, eds., Longman Scientific & Technical, Harlow, UK, 1994, pp. 13–51.
[10] S. C. Brenner and L. R. Scott, *The Mathematical Theory of Finite Element Methods*, Springer-Verlag, New York, 1994.
[11] F. Brezzi and M. Fortin, *Mixed and Hybrid Finite Element Methods*, Springer-Verlag, New York, 1991.
[12] Z. Chen and T. Y. Hou, *A mixed multiscale finite element method for elliptic problems with oscillating coefficients*, Math. Comp., 72 (2003), pp. 541–576.
[13] M. A. Christie, *Tenth SPE comparative solution project: A comparison of upscaling techniques*, SPE Reservoir Evaluation & Engineering, 4 (2001), pp. 308–317.
[14] Y. Efendiev, J. Galvis, and X.-H. Wu, *Multiscale finite element methods for high-contrast problems using local spectral basis functions*, J. Comput. Phys., 230 (2011), pp. 937–955.
[15] Y. R. Efendiev, T. Y. Hou, and X.-H. Wu, *Convergence of a nonconforming multiscale finite element method*, SIAM J. Numer. Anal., 37 (2000), pp. 888–910.
[16] B. Ganis and I. Yotov, *Implementation of a mortar mixed finite element method using a multiscale flux basis*, Comput. Methods Appl. Mech. Engrg., 198 (2009), pp. 3989–3998.
[17] D. Gilbarg and N. S. Trudinger, *Elliptic Partial Differential Equations of Second Order*, Springer-Verlag, Berlin, 1983.
[18] R. Glowinski and M. F. Wheeler, *Domain decomposition and mixed finite element methods for elliptic problems*, in Proceedings of the First International Symposium on Domain Decomposition Methods for Partial Differential Equations, R. Glowinski et al., eds., SIAM, Philadelphia, 1988, pp. 144–172.
[19] I. G. Graham and R. Scheichl, *Robust domain decomposition algorithms for multiscale PDEs*, Numer. Methods Partial Differential Equations, 23 (2007), pp. 859–878.
[20] P. Grisvard, *Elliptic Problems in Nonsmooth Domains*, Pitman, Boston, 1985.
[21] T. Y. Hou and X. H. Wu, *A multiscale finite element method for elliptic problems in composite materials and porous media*, J. Comput. Phys., 134 (1997), pp. 169–189.
[22] T. Y. Hou, X.-H. Wu, and Z. Cai, *Convergence of a multiscale finite element method for elliptic problems with rapidly oscillating coefficients*, Math. Comp., 68 (1999), pp. 913–943.
[23] V. V. Jikov, S. M. Kozlov, and O. A. Oleĭnik, *Homogenization of Differential Operators and Integral Functions*, Springer-Verlag, New York, 1994.
[24] J. V. Lent, R. Scheichl, and I. G. Graham, *Energy minimizing coarse spaces for two-level Schwarz methods for multiscale PDEs*, Numer. Linear Algebra Appl., 16 (2009), pp. 775–799.
[25] S. P. MacLachlan and J. D. Moulton, *Multilevel upscaling through variational coarsening*, Water Resour. Res., 42 (2006), W02418.
[26] T. P. Mathew, *Domain Decomposition and Iterative Refinement Methods for Mixed Finite Element Discretizations of Elliptic Problems*, Ph.D. thesis, Tech. Rep. 463, Courant Institute of Mathematical Sciences, New York University, New York, NY, 1989.
[27] S. Moskow and M. Vogelius, *First-order corrections to the homogenized eigenvalues of a periodic composite medium: A convergence proof*, Proc. Roy. Soc. Edinburgh Sect. A, 127 (1997), pp. 1263–1299.
[28] J. D. Moulton, J. E. Dendy, and J. M. Hyman, *The black box multigrid numerical homogenization algorithm*, J. Comput. Phys., 142 (1998), pp. 80–108.
[29] J. M. Nordbotten and P. E. Bjørstad, *On the relationship between the multiscale finite-volume method and domain decomposition preconditioners*, Comput. Geosci., 12 (2008), pp. 367–376.
[30] C. Pechstein and R. Scheichl, *Robust FETI solvers for multiscale elliptic PDEs*, in Scientific Computing in Electrical Engineering (SCEE 2008), Math. Ind. 2010, Springer, Berlin, 2009, pp. 421–428.
[31] G. Pencheva, M. Vohralik, M. F. Wheeler, and T. Wildey, *Robust a posteriori error control and adaptivity for multiscale, multinumerics, and mortar coupling*, SIAM J. Numer. Anal., accepted.
[32] G. Pencheva and I. Yotov, *Balancing domain decomposition for mortar mixed finite element methods*, Numer. Linear Algebra Appl., 10 (2003), pp. 159–180.
[33] R. A. Raviart and J. M. Thomas, *A mixed finite element method for 2nd order elliptic problems*, in Mathematical Aspects of Finite Element Methods, I. Galligani and E. Magenes, eds., Lecture Notes in Math. 606, Springer, Berlin, 1977, pp. 292–315.

[34] J. E. Roberts and J.-M. Thomas, *Mixed and hybrid methods*, in Handbook of Numerical Analysis, Vol. II, P. G. Ciarlet and J. L. Lions, eds., North–Holland, Amsterdam, 1991, pp. 523–639.

[35] A. Sandvin, J. M. Nordbotten, and I. Aavatsmark, *Multiscale mass-conservative domain-decomposition preconditioners for elliptic problems on irregular grids*, Comput. Geosci., 15 (2011), pp. 587–602.

[36] C. D. White and R. N. Horne, *Computing absolute transmissibility in the presence of fine-scale heterogeneity*, in Proceedings of the Ninth SPE Symposium on Reservoir Simulation, Society of Petroleum Engineers, Allen, TX, 1987, pp. 209–220.

[37] J. Xu and L. Zikatanov, *On an energy minimizing basis for algebraic multigrid methods*, Comput. Vis. Sci., 7 (2004), pp. 121–127.

[38] I. Yotov, *Mixed Finite Element Methods for Flow in Porous Media*, Ph.D. thesis, Rice University, Houston, TX, 1996.